

SIMULATING CLIFFORD CIRCUITS WITH GAUSSIAN ELIMINATION

YUCHEN PANG AND EDGAR SOLOMONIK *

Abstract. Quantum circuits are considered more powerful than classical circuits and require exponential resources to simulate classically. Clifford circuits are a special class of quantum circuits that can be simulated in polynomial time but still show important quantum effects such as entanglement. In this work, we present an algorithm that simulates Clifford circuits by performing Gaussian elimination on a modified adjacency matrix derived from the circuit structure. Our work builds on an ZX-calculus tensor network representation of Clifford circuits that reduces to quantum graph states. We give a concise formula of amplitudes of graph states based on the LDL decomposition of matrices over $\text{GF}(2)$, and use it to get efficient algorithms for strong and weak simulation of Clifford circuits using tree-decomposition-based fast LDL algorithm. The complexity of our algorithm matches the state of art for weak graph state simulation and improves the state of art for strong graph state simulation by taking advantage of Strassen-like fast matrix multiplication. Our algorithm is also efficient when computing many amplitudes or samples of a Clifford circuit. Further, our amplitudes formula provides a new characterization of locally Clifford equivalent graph states as well as an efficient protocol to learn graph states with low-rank adjacency matrices.

Key words. Quantum computation, Clifford circuit, ZX-calculus, Tree decomposition, Gauss-Jordan elimination, Locally Clifford equivalent graph states, Graph state learning

MSC codes. 68Q12, 81P68, 15A09, 05C50

1. Introduction. Circuits consisting of Clifford gates (e.g. Hadamard gate, CZ gate, and the phase gate $R_Z(\pi/2)$) are of wide interest in quantum computing. This gate set would be universal for quantum computing provided inclusion of T gates (i.e. the phase gate $R_Z(\pi/4)$). Despite this restriction, circuits consisting of only Clifford gates (Clifford circuits) suffice to express important quantum circuits, such as stabilizer codes for error correction, and graph states, which have shown to provide an asymptotic depth advantage over any classical circuit [8] (the first quantum advantage result). In addition, Clifford circuits are known to admit polynomial-time simulation algorithms. This celebrated result is known as the Gottesman-Knill theorem [1, 22]. A mathematical intuition for this result is that any n -qubit Clifford state can be associated with an n -dimensional quadratic form [16].

The problem of Clifford circuit simulation can be defined as follows.

DEFINITION 1.1 (Clifford circuit simulation). *Let U be an n -qubit Clifford circuit. The strong simulation of U takes any $x \in \{0, 1\}^n$ as input, and outputs $\langle x|U|0^n\rangle$. The weak simulation of U samples $x \in \{0, 1\}^n$ according to the distribution $P(x) = |\langle x|U|0^n\rangle|^2$.*

Here we adopt the bra-ket notation from physics, where $\langle x|$ and $|0^n\rangle$ can be viewed as row and column vectors of size 2^n respectively and U can be viewed as a 2^n -by- 2^n matrix. Then $\langle x|U|0^n\rangle$ represents the inner product between $\langle x|$ and $U|0^n\rangle$. However, as mentioned above, such matrices and vectors in Clifford circuits admits polynomial-sized representation due to the Gottesman-Knill theorem.

The Clifford circuit simulation problem is closely related to basic linear algebra problems such as matrix-matrix multiplication and linear system solving. State of the art simulation algorithms for Clifford circuits [19, 20, 30] are based on an algebraic formalism known as stabilizer tableaux [7]. A tableau encodes an n -qubit Clifford

*Siebel School of Computing and Data Science, University of Illinois Urbana-Champaign, Urbana, IL 61801, USA (yuchenp2@illinois.edu, solomon2@illinois.edu)

unitary using a pair of matrices and vectors of size $2n$. It has been shown that all Clifford circuit operations such as gate applications and measurements could all be implemented as standard matrix operations on tableaux, where the most costly part is matrix-matrix products [20]. From the perspective of complexity, it is known that simulating Clifford circuits is complete for the complexity class $\oplus L$ [1], which is the complexity class of solving linear systems over \mathbb{F}_2 [13]. An algorithm to solve symmetric linear systems over \mathbb{F}_2 with zero diagonals via graph state simulation is proposed by Gosset et al. [20, Theorem 26]. Our work can be viewed as the other direction of this reduction. In particular, we provide a complete reduction from Clifford circuit simulation problem to the LDL decomposition of a symmetric matrix over \mathbb{F}_2 and give time complexities of circuit simulation based on the fast LDL algorithm [32]. Our algorithm performs better than previous algorithms when calculating many amplitudes/samples by utilizing the Strassen-like fast matrix multiplication.

To represent the Clifford circuit as a matrix so that an LDL decomposition of it gives the simulation result, we leverage a modern formalism for quantum circuits known as ZX-calculus. In particular, we use a canonical form for circuits derived in this formalism known as a graph-like ZX-diagram [17], and then an n -qubit circuit consisting of m gates could be converted to a *phased graph state* with $N = O(m + n)$ vertices. This reduction is described in section 3.

The core of this paper is the analysis of phased graph states and the corresponding simulation algorithm. Phased graph state are defined as generalized graph states characterized by matrices in the set

$$\mathbb{J}_n = \{A \in \mathbb{Z}_4^{n \times n} \mid A = A^T, O(A) \in \mathbb{F}_2^{n \times n}\},$$

where $O(A)$ is off-diagonals of A and informally we treat $\mathbb{Z}_4 = \{0, 1, 2, 3\}$ and $\mathbb{F}_2 = \{0, 1\}$. For $A \in \mathbb{J}_n$, the phased graph state $|A\rangle$ is given by

$$|A\rangle = \bigotimes_{j=1}^n \check{Z}^{a_{jj}} |G\rangle,$$

where $\check{Z} = R_z(-\pi/2)$ is a phase gate, a_{jj} is the j 'th diagonal element of A , and $|G\rangle$ is the standard graph state whose adjacency matrix is $O(A)$.

In section 4, we define a generalized Gauss-Jordan elimination process on $A \in \mathbb{J}_n$ and show that this process corresponds to a series of vertex and edge complementations [14, 18, 37] of $|G\rangle$. Then we provide a simple and explicit formula for the amplitudes of Hadamard-transformed phased graph states as following.

THEOREM 1.2 (Informal form of Theorem 4.5). *Let $A \in \mathbb{J}_n$. Then we have*

$$(1.1) \quad \langle x | H^{\otimes n} |A\rangle = \begin{cases} 2^{-k/2} i^{-(x+v)^T B(x+v)} & x \oplus w \in \text{span}(\omega_1(A)) \\ 0 & \text{otherwise} \end{cases}$$

where $\omega_1(A) = A \bmod 2$, k is rank of $\omega_1(A)$ over \mathbb{F}_2 , and $B \in \mathbb{J}_n$, $w \in \mathbb{F}_2^n$, $v \in \mathbb{F}_2^n$ could be calculated along with an LDL factorization of $\omega_1(A)$. In particular, if the leading block of A , A_{11} , is full rank and we have $\text{rank}(A) = \text{rank}(A_{11})$, then B satisfies

$$(1.2) \quad \omega_1(B) = \begin{bmatrix} A_{11}^\# & B_{21}^T \\ B_{21} & 0 \end{bmatrix}, \quad B_{21} = \omega_1(A_{21}A_{11}^\#),$$

where $A_{11}^\#$ is the inverse of A_{11} over \mathbb{F}_2 .

Prior works have observed that these can be computed by Gaussian elimination [1], but we are not aware of a prior corresponding explicit algebraic expression for them. This formula not only allows us to derive simulation algorithms using standard linear algebra routines, but also has other theoretical implications as discussed in [section 7](#).

In [section 5](#), we give an algorithm to solve the phased graph state simulation problem based on [Theorem 1.2](#) and the tree-decomposition-based fast LDL algorithm [32]. The phased graph state simulation problem is defined as following.

DEFINITION 1.3 (Phased graph state simulation). *Let $A \in \mathbb{J}_n$. The strong simulation of $|A\rangle$ takes any $x \in \mathbb{F}_2^n$ as input and calculates*

$$(1.3) \quad \langle x | H^{\otimes n} | A \rangle.$$

The weak simulation of $|A\rangle$ takes as input $S \subseteq [n]$ and $y \in \mathbb{F}_2^n$ as input, and samples $x \in \mathcal{X}_{S,y} = \{x \in \mathbb{F}_2^n \mid \forall i \in S, x_i = y_i\}$ according to the distribution

$$(1.4) \quad \forall x \in \mathcal{X}_{S,y}, p(x) \propto |\langle x | H^{\otimes n} | A \rangle|^2.$$

By expressing the dominant computations in the simulation task as matrix multiplications, our algorithm exploits the sparsity structure of the graph and the efficiency of fast matrix multiplication, achieving the following time complexity.

THEOREM 1.4 (Summary of [Theorem 5.4](#), [Theorem 5.5](#) and [Theorem 5.6](#)). *Consider any $y \in \mathbb{F}_2^n$, $S \subseteq [n]$, $A \in \mathbb{J}_n$ and a given tree decomposition of the graph corresponding to A with width τ . Let $\ell = n - |S|$. Then strong simulation of A with $k \in \mathbb{N}$ inputs from $\mathcal{X}_{S,y}$ or weak simulation of A for k samples from $\mathcal{X}_{S,y}$ takes $O(n\tau^{\omega-1} + \min(kn\tau^{\omega-2}, \ell n\tau^{\omega-2} + k\ell^{\omega-1}))$ time¹.*

In [section 6](#), we apply our algorithm for phased graph state simulation to other simulation problems such as graph state simulation, Clifford circuit simulation, and Clifford+T circuit simulation. These include the following results. In [subsection 6.1](#), we solve the graph state simulation problem [20] in the following complexity.

THEOREM 1.5 (Restatement of [Theorem 6.3](#)). *Let G be a graph with n vertices and a tree decomposition of G with width τ is given. Then the strong/weak simulation of $|G\rangle$ for $k \in \mathbb{N}$ amplitudes/samples could be solved in $O(n\tau^{\omega-1} + kn\tau^{\omega-2})$ time.*

When $k = 1$, this matches the state of art for weak simulation [20] and improves the previous $O(n\tau^2)$ complexity for strong simulation (with phase) [24]. Our algorithm can also efficiently compute many amplitudes/samples of a fixed graph state, which is not explicitly considered in previous literature. In [subsection 6.2](#), we apply our algorithm to Clifford circuit simulation and get the following complexity based on treewidth of the circuit.

THEOREM 1.6 (Restatement of [Theorem 6.4](#)). *Let U be a Clifford circuit with n qubits and m gates, each of which acts on at most 2 qubits, for $m = \Omega(n)$, and a tree decomposition of the circuit with width τ is given. Then strong/weak simulation of U for $k \in \mathbb{N}$ amplitudes/samples could be solved in $O(m\tau^{\omega-1} + \min(km\tau^{\omega-2}, mn\tau^{\omega-2} + kn^{\omega-1}))$ time.*

Since every n -qubit circuit has a simple tree decomposition of width $O(n)$, our algorithm can simulate any Clifford circuit in $O(mn^{\omega-1} + kn^{\omega-1})$ time. We compare our algorithm with previous Clifford circuit simulation algorithms in [Table 6.1](#) and show

¹ ω denotes the matrix multiplication exponent.

that our algorithm performs better when $m \gg n^{\omega-1}$ and $k \gg m$. In [subsection 6.3](#), we consider the strong simulation of general Clifford+T circuits, we show that the LDL factorization can be used in conjunction with stabilizer decompositions of T gates, obtaining an exact algorithm that improves the previous work [\[24\]](#) in strong simulation of planar Clifford+T circuits. Our algorithm slightly improves upon the scaling of state-of-the-art approximation algorithms with respect to T gate count [\[7\]](#).

In [section 7](#), we present other applications of the amplitudes formula in [Theorem 1.2](#). In [subsection 7.1](#), we give a characterization of locally Clifford (LC) equivalent graph states based on the generalized Gauss-Jordan process as presented in the following theorem.

THEOREM 1.7 (Restatement of [Theorem 7.1](#)). *Graph states with adjacency matrices \bar{A} and \bar{B} are locally equivalent, iff there exist permutation matrices P, Q , diagonal matrices D, E , and some $k \geq 0$ such that $A = P^T(\bar{A} + D)P$, $B = Q^T(\bar{B} + E)Q$,*

$$\text{and for } A_{11} \in \mathbb{F}_2^{k \times k}, B = \begin{bmatrix} A_{11}^\# & \omega_1(A_{21}A_{11}^\#)^T \\ \omega_1(A_{21}A_{11}^\#) & \omega_1(A_{22} - A_{21}A_{11}^\#A_{12}) \end{bmatrix}.$$

Based on [Theorem 1.7](#), we give a linear upper bound for each orbit of LC equivalent graph states [\[2\]](#). In [subsection 7.2](#), we provide an efficient protocol to learn graph states with low-rank adjacency matrices.

1.1. Related works. Our amplitude formula in [Theorem 1.2](#) is closely related the quadratic-form-expansion (QFE) method for Clifford circuit simulation [\[15\]](#), which is covered in more detail in [subsection 2.6.1](#). Here, we highlight several key differences between our algorithm and the QFE method. Firstly, the QFE method represents a stabilizer state with a quadratic form in [\(2.1\)](#) and simulates the circuit by applying gates and measurements in order. In comparison, our method views the whole circuit as a graph and exploits its overall structure. Secondly, the QFE method designs dedicated algorithms that transforms the quadratic form to implement gate applications and measurements on arbitrary stabilizer states. In contrast, our method focuses on a subset of stabilizer states that admit richer structures, namely phased graph states. This allows us to relate vertex and edge complementations to standard Gaussian elimination routines and utilize fast algorithms based on Strassen’s fast matrix multiplication. This leads to the difference in time complexities as shown in [Table 6.1](#).

Also, the phased graph state simulation problem we solve can be viewed as a variant of the graph state simulation problem studied in [\[20\]](#) and [\[24\]](#). Our algorithm matches the complexity of theirs for weak simulation and improves the time complexity for strong simulation as discussed in [subsection 6.1](#). In addition, Gosset et al. [\[20, 24\]](#) also consider the Clifford circuit simulation problem by converting the circuit to a graph state in a similar way as ours. In particular, they consider the connectivity graph of qubits and bound the treewidth of depth- d circuits using the treewidth of the qubit-connectivity graph. In this work, we focus on the graph structure of circuits and give a specific circuit-to-graph reduction that allows the reduction from circuit simulation to LDL decomposition. This leads to algorithms for different scenarios with different complexities, which are further discussed in [subsection 6.1](#) and [subsection 6.2](#).

2. Preliminaries and Notations.

2.1. Matrix-related notations. We use uppercase letters such as A, B, U to represent matrices, operators, and quantum circuits. Lowercase letters like x, y represent vectors. Lowercase letters with subscripts are used to denote elements in the

corresponding matrix or vector. For example, v_i denotes the i 'th element in v , and a_{ij} denotes the element in the i 'th row and j 'th column in A .

To specify the range of indices, we define $[n] = \{i \in \mathbb{Z} \mid 1 \leq i \leq n\}$. Also, we use the abbreviation $[1..n] = [n]$. Given $S \subseteq [n]$ and $y \in \mathbb{F}_2^n$, we define $\mathcal{X}_{S,y} = \{x \in \mathbb{F}_2^n \mid \forall i \in S, x_i = y_i\}$ to represent vectors that agree with y over the indices in S . In addition, we use \mathbb{F}^S to denote the set of vectors over \mathbb{F} indexed by elements in S .

The identity matrix is represented by I when its size is clear in the context. Otherwise, we use I_n to denote the identity matrix of size n . The elementary vector e_i indicates the i 'th vector in standard basis, i.e. the i 'th row/column vector of I . The length of e_i should always be clear in the context.

The vector given by the diagonal of A is represented by $d(A)$, while $D(A)$ refers to the matrix that only contains the diagonal part of A . Additionally, we use $O(A)$ to denote the matrix that contains only the off-diagonal part of A . For a vector in $v \in \mathbb{Z}^n$, let $D(v)$ be the diagonal matrix with diagonal equal to v .

The transpose of a matrix A is denoted as A^T and the conjugate transpose of a complex matrix A is denoted as A^\dagger .

To describe a local operator $U : V \rightarrow V$ acting on the j 'th component of a tensor product space $V^{\otimes n}$, we define $U^{(j)} = I \otimes \dots \otimes U \otimes \dots \otimes I$, where U is the j 'th operator and all other $n - 1$ operators are identities. Similarly, we use $W^{(i,j)}$ to denote an operator $W : V \otimes V \rightarrow V \otimes V$ that acts on the i 'th and j 'th component of $V^{\otimes n}$. Also, for $v \in \mathbb{Z}^n$, we define $U^v = \bigotimes_{j=1}^n U^{v_j}$.

The matrix multiplication exponent is denoted by ω . That is, we assume the cost of multiplying two matrices of size $n \times n$ is $O(n^\omega)$, where $2 < \omega < 2.372$ [34, 38].

2.2. Matrices over \mathbb{Z}_4 and \mathbb{F}_2 . Let \mathbb{Z}_4 be the ring of integers modulo 4 with elements $\{0, 1, 2, 3\}$. Let $\omega_i(x) = \lfloor x/2^{i-1} \rfloor \bmod 2$ for any integer scalar, vector, or matrix x over \mathbb{Z}_4 , which calculates the i 'th bit of x in binary representation.

Let $\mathbb{F}_2 = \{0, 1\} \subset \mathbb{Z}_4$ and define $a \oplus b = \omega_1(a + b)$. Then $(\mathbb{F}_2, \oplus, \cdot)$ is the finite field of size 2. For $A \in \mathbb{F}_2^{n \times n}$, we use $A^\#$ to denote the inverse of A over \mathbb{F}_2 (by A^{-1} we will have in mind the inverse of $A \in \mathbb{Z}^{n \times n}$ over \mathbb{Z} if it exists).

For matrix $A \in \mathbb{F}_2^{n \times n}$, we use $\text{rank}(A)$ and $\text{span}(A)$ to refer to the rank and column span of A over \mathbb{F}_2 .

The LDL decomposition over \mathbb{F}_2 is defined as following to characterize the Gaussian elimination process on symmetric matrices over \mathbb{F}_2 .

DEFINITION 2.1 (LDL decomposition over \mathbb{F}_2). *Let $A \in \mathbb{F}_2^{n \times n}$ be symmetric. Then the triple (P, L, D) is an LDL decomposition of A over \mathbb{F}_2 if*

1. $A = \omega_1(PLDL^T P^T)$;
2. $P \in \mathbb{F}_2^{n \times n}$ is a permutation matrix;
3. $L \in \mathbb{F}_2^{n \times n}$ is unit-diagonal and lower-triangular;
4. $D \in \mathbb{F}_2^{n \times n}$ is block-diagonal with blocks 0, 1, or $\begin{bmatrix} 0 & 1 \\ 1 & 0 \end{bmatrix}$;
5. For each i such that $\begin{bmatrix} d_{ii} & d_{i(i+1)} \\ d_{(i+1)i} & d_{(i+1)(i+1)} \end{bmatrix} = \begin{bmatrix} 0 & 1 \\ 1 & 0 \end{bmatrix}$, $l_{(i+1)i} = 0$.

An LDL decomposition of a symmetric matrix always exists and can be constructed via standard Gaussian elimination. The use of such a decomposition in applications dates back to work on integer factoring in the 1970s [25, 28].

When A is not full rank, we sometimes use the reduced LDL decomposition of it.

DEFINITION 2.2 (Reduced LDL decomposition over \mathbb{F}_2). *Let $A \in \mathbb{F}_2^{n \times n}$ be sym-*

metric with rank r . Then (P, L, D) is a reduced LDL decomposition of A over \mathbb{F}_2 , where P, L, D are defined the same as in [Definition 2.1](#), except that

- $L \in \mathbb{F}_2^{n \times r}$ is unit-diagonal and lower-trapezoidal;
- $D \in \mathbb{F}_2^{r \times r}$ is block-diagonal with blocks 1, or $\begin{bmatrix} 0 & 1 \\ 1 & 0 \end{bmatrix}$.

2.3. Tree decomposition and treewidth. The complexity results in this work rely on Gaussian elimination algorithms based on tree decompositions [\[32\]](#), which is introduced below.

DEFINITION 2.3 (Tree decomposition). *A tree decomposition of a graph $G = (V, E)$ is a tree $T = (V_T, E_T)$ such that each node $B \in V_T$ is a bag, $B_t \subseteq V$, and the following conditions are satisfied,*

- For each $v \in V$, there exists $B \in V_T$ such that $v \in B$,
- For each $(u, v) \in E$, there exists $B \in V_T$ such that $\{u, v\} \subseteq B$;
- For each $v \in V$, $\{B \in V_T \mid v \in B\}$ forms a connected subtree of T .

Also, the width of T is defined as $(\max_{B \in V_T} |B| - 1)$.

The treewidth of a graph could then be defined as follows.

DEFINITION 2.4 (Treewidth). *The treewidth of a graph G , or $tw(G)$, is the smallest number w such that any tree decomposition of G has width at least w .*

2.4. Quantum circuits. In this section, we introduce the necessary definitions and concepts about quantum circuits that are used in this paper. For a more detailed introduction to quantum computation and related topics, we refer our readers to [\[29\]](#).

Qubits are quantum analog of bits in classical computation. Each qubit could be defined as a normalized vector in \mathbb{C}^2 up to a complex phase factor, while an n -qubit quantum state is defined as a normalized vector in n -fold tensor product of \mathbb{C}^2 up to a phase factor. By convention, we will use $|\psi\rangle$ to represent such vectors, where ψ is a label depending on the context, and use $\langle\psi|$ to represent the conjugate transpose of $|\psi\rangle$. For example, some commonly used quantum states are denoted as

$$|0\rangle = \begin{bmatrix} 1 \\ 0 \end{bmatrix}, \quad |1\rangle = \begin{bmatrix} 0 \\ 1 \end{bmatrix}, \quad |+\rangle = \frac{1}{\sqrt{2}} \begin{bmatrix} 1 \\ 1 \end{bmatrix}, \quad |-\rangle = \frac{1}{\sqrt{2}} \begin{bmatrix} 1 \\ -1 \end{bmatrix}.$$

The states $|0\rangle$ and $|1\rangle$ are called the *computational basis* for a qubit. For multiple qubits, the computational basis states are obtained via tensor products, which we express with the notation $|b\rangle = |b_1\rangle \otimes \cdots \otimes |b_n\rangle$ for $b \in \{0, 1\}^n$.

A quantum circuit (without measurements) describes quantum computation with a series of quantum gates, where each gate is a unitary acting on a subset of qubits. Therefore, a quantum gate on n qubits can be represented as a 2^n -by- 2^n matrix. For example, some quantum gates used in this paper are

$$X = \begin{bmatrix} 0 & 1 \\ 1 & 0 \end{bmatrix}, \quad Y = \begin{bmatrix} 0 & -i \\ i & 0 \end{bmatrix}, \quad Z = \begin{bmatrix} 1 & 0 \\ 0 & -1 \end{bmatrix}, \quad H = \frac{1}{\sqrt{2}} \begin{bmatrix} 1 & 1 \\ 1 & -1 \end{bmatrix},$$

$$R_z(\theta) = \begin{bmatrix} 1 & 0 \\ 0 & e^{i\theta} \end{bmatrix}, \quad R_x(\theta) = HR_z(\theta)H, \quad U_{CZ} = \begin{bmatrix} 1 & 0 & 0 & 0 \\ 0 & 1 & 0 & 0 \\ 0 & 0 & 1 & 0 \\ 0 & 0 & 0 & -1 \end{bmatrix},$$

where X, Y and Z are known as Pauli matrices and H is known as the Hadamard gate. Note that similar to quantum states, quantum gates differ by a phase factor are equivalent, i.e. U and $e^{i\theta}U$ for $\theta \in \mathbb{R}$ are equivalent.

Also, we define the following abbreviation,

$$\hat{Z} = R_z(\pi/2), \quad \check{Z} = R_z(-\pi/2), \quad \hat{X} = R_x(\pi/2), \quad \check{X} = R_x(-\pi/2).$$

Note that $\hat{Z} = \check{Z}^{-1}$ and $\hat{Z}^2 = \check{Z}^2 = Z$, and similar relations hold for \hat{X} , \check{X} and X .

Measuring an n -qubit quantum state $|\psi\rangle$ in computational basis corresponds to sample a binary string $b \in \{0, 1\}^n$ from the distribution $P(b) = |\langle b|\psi\rangle|^2$. Typically, quantum simulation algorithms work on emulating measurements (a.k.a. weak simulation), or computing one or more amplitudes (or just magnitudes of amplitudes) of a state $|\psi\rangle$ obtained by executing a quantum circuit (a.k.a. strong simulation). The latter could be used as a subroutine to solve the former problem [9].

2.5. Graph states. Let $G = (V, E)$ be a simple undirected graph with vertices $V(G) = V$ and edges $E(G) = E$. We use ij to denote the edge $\{i, j\} \in E$. For $v \in V$, we use $N(v)$ to represent its neighbors, i.e. $N(v) = \{u \mid uv \in E\}$. Additionally, we use $G \setminus S$ for some $S \subset V$ to represent the subgraph induced by $V \setminus S$. The adjacency matrix of G is defined as a symmetric matrix $A \in \mathbb{F}_2^{n \times n}$ with zero diagonals and $a_{ij} = 1$ iff $ij \in E$. Moreover, to simplify the notations of matrices and tensor product spaces related to G , we assume V are ordered and indexed by $[n] = \{1, \dots, n\}$. Then graph states can be defined as follows.

DEFINITION 2.5 (Graph state). *Let $G = (V, E)$ be a simple undirected graph. Then the corresponding graph state is defined by $|G\rangle = \prod_{ij \in E} U_{CZ}^{(i,j)} |+\rangle^{\otimes |V|}$.*

Next, we introduce two operations on graphs, namely *vertex complementation* and *edge complementation*, that can be implemented on graph states with only local gates. They are also known as local complementation and edge-local complementation respectively in literature [5]. Let Δ denote symmetric difference, $K(A) = \{uv \mid u, v \in A\}$, and $K(A, B) = \{uv \mid u \in A, v \in B\}$ for some vertices sets A and B .

THEOREM 2.6 (Vertex complementation [14, 37]). *Let $G = (V, E)$ be a simple undirected graph and $i \in V$ and $\tau_i(G) = (V, E \Delta K(N(i)))$ denote the local complementation of G at vertex v . Then we have*

$$|G\rangle = \check{X}^{(i)} \prod_{j \in N(i)} \hat{Z}^{(j)} |\tau_i(G)\rangle.$$

THEOREM 2.7 (Edge complementation, Proposition 3.1 in [18]). *Let $G = (V, E)$ be a simple undirected graph and $ij \in E$ and $\epsilon_{ij}(G) = \tau_i \circ \tau_j \circ \tau_i(G)$ denote the edge complementation of G along ij . Then we have*

$$|G\rangle = H^{(i)} H^{(j)} \prod_{k \in N(i) \cap N(j)} Z^{(k)} |\epsilon_{ij}(G)\rangle.$$

We note that $\epsilon_{ij}(G)$ could be alternatively defined as (V, F) , where F is obtained by: (1) replacing E with $E \Delta (K(A, B) \cup K(A, C) \cup K(B, C))$, where $A = N(i) \setminus N(j)$, $B = N(j) \setminus N(i)$ and $C = N(i) \cap N(j)$; (2) and exchanging the neighbors of i and j .

Also, it is widely known that the amplitudes of a graph state in computational basis has a simple formula.

LEMMA 2.8 ([11]). *Let $|G\rangle$ be an n -qubit graph state with adjacency matrix A and $x \in \mathbb{F}_2^n$. Then*

$$\langle x|G\rangle = 2^{-n/2} (-1)^{\frac{1}{2}x^T A x}.$$

Note that $x^T A x$ is always even since A is an adjacency matrix.

2.6. Clifford circuits and stabilizer states. Clifford circuits are a subset of quantum circuits that can be represented by the gate set $\{H, \hat{Z}, U_{CZ}\}$. It is known

that such circuits can be simulated in polynomial time on classical computers by the Gottesman-Knill theorem [1, 16, 20].

The states generated by Clifford circuits are called *stabilizer states*, since such state can be identified with a group of 2^n Pauli operators that stabilize it² [10, 21, 22]. These Pauli operators are known as stabilizers and each stabilizer is a signed n -fold tensor product of $\{I, X, Y, Z\}$. The group operation is defined to be multiplication because if A and B are both stabilizers of a state, then AB is also its stabilizer. Since this group of 2^n stabilizers can be represented by a subset of size n that generates it, each stabilizer state can be also be identified by this generating set. In other words, each stabilizer state can be represented by n signed Pauli operators $\{S_1, \dots, S_n\}$ that are independent and commuting. Here, the independency means that $S_i S_j \neq \pm S_k$ for any different $i, j, k \in [n]$.

Furthermore, let Q be a Clifford circuit applied on a state $|\psi\rangle$ stabilized by $\{S_1, \dots, S_n\}$. Then we have

$$Q|\psi\rangle = (QS_j Q^{-1})Q|\psi\rangle, \quad \forall j = 1, \dots, n.$$

Since $QS_j Q^{-1}$ is still a signed Pauli operator, Q can be viewed as a mapping from one group of 2^n stabilizers to another group of 2^n stabilizers. Such a mapping could be fully described by specifying the images of $2n$ independent Pauli operators.

The widely-used *tableau method* [1] utilizes this fact to represent Clifford circuits efficiently. The tableau method describes Q by its images of X^{e_j} and Z^{e_j} for $j = 1, \dots, n$. These images are encoded in the following matrix,

$$\begin{bmatrix} \bar{X} & \bar{Z} & s \\ \tilde{X} & \tilde{Z} & r \end{bmatrix},$$

where $\bar{X}, \bar{Z}, \tilde{X}, \tilde{Z} \in \{0, 1\}^{n \times n}$, $r, s \in \{0, 1\}^n$, and

$$QX^{e_j}Q^{-1} = (-1)^{s_j} \bigotimes_{k=1}^n P^{(\bar{z}_{jk}, \bar{x}_{jk})},$$

$$QZ^{e_j}Q^{-1} = (-1)^{r_j} \bigotimes_{k=1}^n P^{(\tilde{z}_{jk}, \tilde{x}_{jk})},$$

for $P^{(0,0)} = I, P^{(1,0)} = Z, P^{(0,1)} = X, P^{(1,1)} = Y$.

A stabilizer state $|\psi\rangle$ can also be represented with a tableau by representing some Q such that $|\psi\rangle = Q|0^n\rangle$ (note that the last n rows of the tableau of Q exactly generates the stabilizers of $|\psi\rangle$). It has been shown that in this representation, circuit composition, amplitude evaluation and measurements can all be reduced to matrix multiplications and cost $O(n^\omega)$ time [1, 20]. Moreover, it is worth mentioning that applying basic Clifford gates such as $\{H, S, U_{CZ}\}$ to a stabilizer state in tableau representation only costs $O(n)$ time [1]. We also list these gate application algorithms in [Algorithm A.1](#).

2.6.1. Other Clifford circuit simulation methods. Besides tableaux, graph states and quadratic form expansions are also used to simulate Clifford circuits in classical polynomial time. We discuss two such methods below.

The graph-state-based method [3] represent a stabilizer state as a graph state with local Clifford operators applied on each vertex. Such representation always exists [37]³. Then gate application and measurements can both be implemented by

²It means $A|\psi\rangle = |\psi\rangle$ that an operator A stabilizes $|\psi\rangle$.

³We also provide an explicit algorithm that transforms a stabilizers to such form in [section A](#).

changing structure of the graph and updating the local operators due to [Theorem 2.6](#). Let n be number of qubits and m be number of gates. Then the time cost of finding the representation of the final state is $O(ndm)$, where $d \leq n$ is the maximal degree of the graph during simulation, and each one-qubit measurement costs $O(d)$ time.

The quadratic-form-expansion methods [\[15\]](#) utilize the fact that an n -qubit stabilizer state can always be written in the following form [\[36\]](#),

$$(2.1) \quad |\psi\rangle = 2^{-r/2} \sum_{x \in \{0,1\}^r} i^{x^T Q x} |(Ax + b) \bmod 2\rangle,$$

where $r \leq n$, $A \in \{0,1\}^{n \times r}$, $b \in \{0,1\}^n$, and symmetric $Q \in \{0,1\}^{n \times n}$. Applying Clifford gates to this representation can be described by matrix operations [\[15\]](#). Then simulating an n -qubit circuit with m gates would cost $O(mn^2)$ time, after which sampling or amplitude computing only takes $O(n^2)$ time.

2.7. Tensor networks. Tensor networks are graphical representation of tensor contractions. The tensor networks used in this paper can be defined as (G, O) . G is a multigraph such that $V(G)$ is a set of contracted tensors and $E(G)$ is the multiset of contracted indices. O is a multiset representing uncontracted indices, which is also known as open edges. For example, the following contraction,

$$(2.2) \quad T_{ijk} = \sum_{\alpha\beta\gamma} A_{ij\alpha\gamma} B_{\alpha\beta} C_{\beta\gamma k}$$

is represented by the graph $G = (\{A, B, C\}, \{\alpha, \beta, \gamma\})$ and $O = \{i, j, k\}$, where

$$i = j = \{A\}, \quad k = C, \quad \alpha = \{A, B\}, \quad \beta = \{B, C\}, \quad \gamma = \{A, C\}.$$

The diagrams of such graphs are known as tensor diagrams. For example, [Figure 2.1](#) shows the tensor diagram of [\(2.2\)](#). When $O = \emptyset$, we call the tensor network as *closed*.

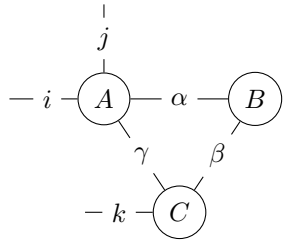


FIGURE 2.1. A tensor diagram representing [\(2.2\)](#)

Tensor networks are a powerful tool in studying many-body quantum systems where high-dimensional tensors are approximated by compact tensor network representation. Also, they play an important role in quantum circuit simulation because quantum circuits can be viewed as tensor networks [\[26\]](#). In this paper, we will focus on the latter application.

2.8. ZX-diagrams. ZX-diagrams are special tensor networks that only contain two types of tensors known as *Z-spiders* and *X-spiders*, respectively [12],

$$Z(\alpha)_{i_1 i_2 \dots i_n} = \begin{cases} 1 & i_1 i_2 \dots i_n = 00 \dots 0 \\ \exp(i\alpha) & i_1 i_2 \dots i_n = 11 \dots 1 \\ 0 & \text{otherwise,} \end{cases}$$

$$X(\alpha) = \prod_{j=1}^n H^{(j)} Z(\alpha),$$

where indices $i_j \in \{0, 1\}$ for $j = 1 \dots n$ and $H^{(j)}$ is the Hadamard matrix applied on the j 'th index. In this paper, we will use white and gray nodes to represent Z- and X-spiders respectively in the diagrams, and when $\alpha = 0$, we omit the 0 inside the node:

$$Z(\alpha) = \text{white spider with } \alpha \text{ inside}, \quad X(\alpha) = \text{gray spider with } \alpha \text{ inside}, \quad \text{white spider with } 0 \text{ inside} = \text{white spider}.$$

ZX-diagrams can be used to represent quantum states and quantum gates. For example, we have the following up to a multiplicative constant factor.

$$(2.3) \quad \begin{aligned} |0\rangle &= \text{white spider with } 0 \text{ inside}, & |1\rangle &= \text{gray spider with } \pi \text{ inside}, & |+\rangle &= \text{white spider with } 0 \text{ inside}, & |-\rangle &= \text{gray spider with } \pi \text{ inside}, \\ Z &= \text{white spider with } \pi \text{ inside}, & X &= \text{gray spider with } \pi \text{ inside}, & S &= \text{white spider with } \frac{\pi}{2} \text{ inside}, & T &= \text{gray spider with } \frac{\pi}{4} \text{ inside}, \\ U_{CZ} &= \text{white spider with } \square \text{ inside} & \text{where } \square &= H = \text{white spider with } \frac{\pi}{2} \text{ inside} - \text{gray spider with } \frac{\pi}{2} \text{ inside} - \text{white spider with } \frac{\pi}{2} \text{ inside}. \end{aligned}$$

Here, we use a square node to represent H gate to simplify the diagram even though it is representable by only Z- and X-spiders. Also, we note that the constant factor is often omitted in ZX-diagrams, because it can be easily calculated along with the diagram itself. In this paper, we also omit these constant factors for simplicity as they would not affect our results.

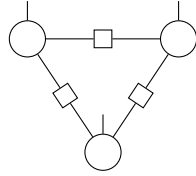
It is worth noting that ZX-diagrams, along with a set of rules that transform them, are complete to describe linear maps between qubits [23]. One of the rules we use in this paper is known as *merge* rule, which says that two connected spiders of the same type can be merged into one with their phases being summed up. A diagram that depicts merge rule is shown below.

$$(2.4) \quad \text{white spider with } \alpha \text{ inside} - \text{white spider with } \beta \text{ inside} = \text{white spider with } \alpha + \beta \text{ inside}$$

For a complete list of rules, we refer our readers to [23].

2.9. Graph states as ZX-diagrams. ZX-diagrams can represent graph states in a convenient way. Let $G = (V, E)$ be a graph, then $|G\rangle$ is represented by a ZX-diagram with $|V|$ Z-spiders of phase 0. Each Z-spider corresponds to a vertex in G , which has an open edge and is connected to its neighbors via a Hadamard node. For example, let K_3 be the complete graph with 3 vertices. The ZX-diagram of $|K_3\rangle$ is

shown below.



The correctness of this representation could be easily seen by rewriting [Definition 2.5](#) using ZX-diagrams.

2.10. Graph-like ZX-diagrams. Due to the natural relation between graph states and ZX-diagrams, *graph-like ZX-diagrams* have been proposed as a canonical form to help analyze and simplify them [17].

DEFINITION 2.9 (Graph-like ZX-diagram). *A ZX-diagram is called graph-like if*

1. *it only contains Z-spiders and Hadamard gates;*
2. *Z-spiders are only connected via Hadamard gates and Hadamard gates are only used to connect Z-spiders;*
3. *Z-spiders and all Hadamard gates connecting them form a simple graph;*
4. *every open edge is incident to a Z-spider and every Z-spider is incident to at most one open edge.*

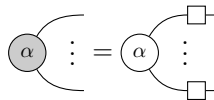
By definition, each graph-like ZX-diagram admits an underlying graph formed by Z-spiders as the *vertices* and Hadamard gates as the *edges*. Note that this graph is different from the graph by viewing the diagram as a tensor network (where Hadamard gates are treated as vertices). However, when considering the treewidth of a graph-like ZX-diagram, both definitions of the underlying graph lead to equivalent tree decompositions and give the same definition of treewidth. Therefore, we will not distinguish them when the context is clear.

Any ZX-diagram is equivalent to a graph-like ZX-diagram [17]. Moreover, it is implicitly shown by the proof of [17, Lemma 3.2] that the complexity of this reduction is linear and the treewidth of the diagram is not increased. These are summarized in the following lemma as a modified version of [17, Lemma 3.2].

LEMMA 2.10. *Let \mathcal{D} be any ZX-diagram with n spiders, m contracted indices and k uncontracted indices. Then \mathcal{D} can be converted to an equivalent graph-like ZX-diagram \mathcal{D}' with at most $(n + 5k)$ vertices and at most $(m + 2k)$ edges in $O(m + n + k)$ time. Moreover, if a tree decomposition with width t of \mathcal{D} is given, one can obtain a tree decomposition of \mathcal{D}' with width at most t in the same time complexity.*

Proof. We restate the algorithm given by the proof of [17, Lemma 3.2] to analyze its time and space complexity. The algorithm takes the following steps to convert \mathcal{D} to \mathcal{D}' .

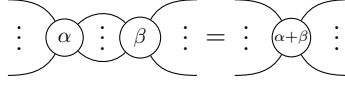
1. Replace all X-spiders with Z-spiders and Hadamards by definition.



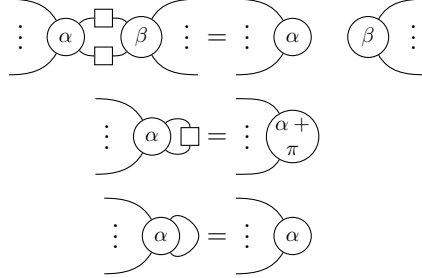
2. Remove adjacent Hadamards since they cancel each other.



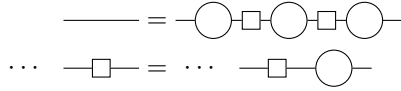
3. Remove edges without Hadamards by merging adjacent Z-spiders.



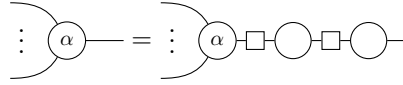
4. Remove parallel Hadamard edges and self loops by using the following rules:



5. For open edges that are not connected to Z-spiders, add dummy spiders to connect them.



6. For multiple open edges connected to one Z-spider, adding dummy spiders to split them.



Note that each step can be completed by traversing the graph once, so the running time is $O(n + m + k)$. Also, note that steps 1 to 4 does not increase the number of vertices/spiders or edges, and step 5 and 6 introduce at most 5 vertices and 2 edges for each uncontracted indices so \mathcal{D}' has at most $(n + 5k)$ vertices and at most $(m + 2k)$ edges. Moreover, consider an arbitrary tree decomposition \mathcal{T} of \mathcal{D} . All graph operations involved in steps 1 to 6 (including merging connected vertices, deleting vertices/edges, and adding chained dummy vertices) transform \mathcal{T} in linear time, and none of these operations increases the width of \mathcal{T} . \square

3. Clifford circuit simulation as phased graph state simulation. In this section, we define phased graph states, and present a reduction from Clifford circuit simulation to phased graph state simulation. This allows us to transform the circuit using vertex and edge complementation (i.e. [Theorem 2.6](#) and [Theorem 2.7](#)) and apply tools from linear algebra to solve the simulation problem in [section 5](#).

To begin with, we define *phased graph states* as a generalization of graph states with arbitrary \tilde{Z} gates applied on each vertex of the graph. Such states can be represented by symmetric matrices whose off-diagonals are over \mathbb{F}_2 and diagonals are over \mathbb{Z}_4 . In particular, consider $A \in \mathbb{Z}_4^{n \times n}$, we define $\Omega_{1,2}(A) = \omega_1(A) + 2\omega_2(D(A))$ and denote $\mathbb{J}_n = \{A \in \mathbb{Z}_4^{n \times n} \mid \Omega_{1,2}(A) = A, A = A^T\}$. Then phased graph states can be defined as follows.

DEFINITION 3.1 (Phased graph state). *Let $A \in \mathbb{J}_n$. Then the phased graph state $|A\rangle$ is defined by $|A\rangle = \tilde{Z}^{d(A)} |G\rangle$, where G is the graph with adjacency matrix $O(A)$.*

Similar notations of phased graph states have been seen in the literature [33,39]. Also, the amplitudes of $|A\rangle$ in computational basis could be obtained as a generalization of Lemma 2.8.

LEMMA 3.2. *Let $A \in \mathbb{J}_n$ and $x \in \mathbb{F}_2^n$. Then $\langle x|A\rangle = 2^{-n/2}(-i)^{x^T A x}$.*

Proof. Note that \check{Z} gates in $|A\rangle$ only introduce a complex phase depending on x and $d(A)$. Then by Definition 3.1 and Lemma 2.8,

$$\langle x|A\rangle = \langle x|\check{Z}^{d(A)}|O(A)\rangle = (-i)^{x^T d(A)} \langle x|O(A)\rangle = 2^{-n/2}(-i)^{x^T A x}. \quad \square$$

We are interested in solving the strong and weak simulation problem for phased graph states defined as follows.

DEFINITION 3.3 (Phased graph state simulation). *Let $A \in \mathbb{J}_n$. The strong simulation of $|A\rangle$ takes any $x \in \mathbb{F}_2^n$ as input and calculates*

$$\langle x|H^{\otimes n}|A\rangle.$$

The weak simulation of $|A\rangle$ takes as input $S \subseteq [n]$ and $y \in \mathbb{F}_2^n$ as input, and samples $x \in \mathcal{X}_{S,y}$ according to the distribution

$$\forall x \in \mathcal{X}_{S,y}, p(x) \propto |\langle x|H^{\otimes n}|A\rangle|^2.$$

Note that we always consider the phased graph states being transformed by Hadamard gates because of two reasons: (1) this is a natural result of Lemma 3.4 as presented below; (2) vertices that are not transformed by Hadamard gates can be efficiently eliminated from the graph as we will discuss in subsection 6.1.

Now we are ready to present the following lemma that reduces Clifford circuit simulation problem as defined in Definition 1.1 to phased graph state simulation as defined in Definition 3.3.

LEMMA 3.4. *Let U be an n -qubit Clifford circuit represented by m gates from the gate set $\{H, \check{Z}, U_{CZ}\}$. Then one can compute a tuple (A, S, y) in $O(m+n)$ time, where $A \in \mathbb{J}_N$ represents a phased graph state for some $N = O(m+n)$, $S \subseteq [n]$ with $|S| = N - n$, and $y \in \mathbb{F}_2^S$, such that*

- *the strong simulation of U for any $x \in \mathbb{F}_2^{[n] \setminus S}$ is equivalent to the strong simulation of $|A\rangle$ with input \tilde{x} such that $\tilde{x}_i = \begin{cases} x_i & i \in [n] \setminus S \\ y_i & i \in S; \end{cases}$*
- *the weak simulation of $|A\rangle$ is equivalent to the weak simulation of $|A\rangle$ with input S and y ;*
- *any tree decomposition of the circuit U with width t can be converted to a tree decomposition of the graph corresponding to A with width at most t .*

Proof. This reduction could be obtained by combining known techniques in ZX calculus. Consider $U|0^n\rangle$, whose ZX-diagram representation could be obtained by connecting small ZX-diagrams that represent each gate in U and $|0\rangle^{\otimes n}$ as given in (2.3). This ZX-diagram contains $O(m+n)$ vertices, $O(m+n)$ edges, and $O(n)$ open edges. By Lemma 2.10, this ZX-diagram could be converted to be graph-like in $O(m+n)$ time, and the resulting graph-like ZX-diagram contains $O(m+n)$ vertices and $O(m+n)$ edges.

Note that the graph-like ZX-diagram from the previous step has n open edges, each of which corresponds to an output qubit of $U|0^n\rangle$. For each output qubit j , we

represent x_j as a ZX-diagram that looks like

$$(3.1) \quad \langle x_j | = \textcircled{x_j\pi} - = \textcircled{x_j\pi} - \square -.$$

Connecting (3.1) to each open edge, we get a graph-like ZX-diagram representing $\langle x|U|0^n\rangle$ and the tree deewidth is not increased. This ZX-diagram contains $N = O(m+n)$ Z-spiders and no open edges, and n of the Z-spiders have phase $x_j\pi$. Moreover, the phases of Z-spiders are all multiples of $\pi/2$ because these phases are all sums of the phases in (2.3) due to the merge rule (2.4).

Next, we will show that the ZX-diagram representing $\langle x|U|0^n\rangle$ from the previous step can be converted to the form of phased graph state simulation.

To begin with, we note that a graph-like ZX-diagram without open edges can be viewed as an inner product between a graph state and tensor product of some one-qubit states: for each Z-spider of phase p_j , one can apply the merge rule (2.4) reversely to split it into two connected Z-spiders, so that one of them has phase p_j and the other inherits the edges associated with the original Z-spider. Then the former spiders represent a tensor product of one-qubit states, while the latter represents a graph state as presented in subsection 2.9. This procedure is illustrated in Figure 3.1.

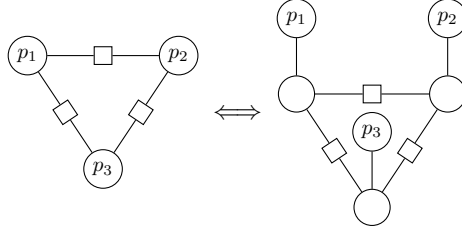


FIGURE 3.1. A graph-like ZX-diagram viewed as an inner product between graph states and a tensor product of one-qubit states. The Z-spiders with phases p_j represent a tensor product of one-qubit states, while the remaining ZX-diagram represents a graph state.

Applying this procedure to the ZX-diagram representing $\langle x|U|0^n\rangle$, we get a graph G with $N = O(m+n)$ vertices and a tensor product of one-qubit states represented by Z-spiders,

$$(3.2) \quad \bigotimes_{j=1}^N \langle \psi_j | = \bigotimes_{j=1}^N \frac{1}{\sqrt{2}} (\langle 0 | + e^{ip_j} \langle 1 |).$$

Since all p_j are multiples of $\pi/2$, let $\tilde{x}_j = \lfloor p_j/\pi \rfloor \bmod 2$ and $a_j = (-2p_j/\pi) \bmod 2$. Then we have

$$(3.3) \quad \langle \psi_j | = \langle 0 | H \hat{Z}^{2\tilde{x}_j - a_j} = \langle 0 | X^{\tilde{x}_j} H \check{Z}^{a_j} = \langle \tilde{x}_j | H \check{Z}^{a_j}.$$

Let $A \in \mathbb{J}_N$ such that $d(A) = a$ and $O(A)$ is the adjacency matrix of G and we have $N = O(m+n)$. The graph-like ZX-diagram representing $\langle \tilde{x}|U|0^n\rangle$ is equal to

$$(3.4) \quad \langle \tilde{x} | H^{\otimes n} \check{Z}^a | G \rangle = \langle \tilde{x} | H^{\otimes n} | A \rangle.$$

Note that by construction, n of the \tilde{x}_j 's are equal to $x_j\pi$. We define S to be the set containing the remaining $N - n$ indices and define $y \in \mathbb{F}_2^S$ such that $y_j = \tilde{x}_j$ for

$j \in S$. Then we have (A, S, y) as stated in the lemma such that the strong and weak simulation of U is equivalent to the strong and simulation of $|A\rangle$. Also, given any tree decomposition of U with width t , a tree decomposition of A of width at most t could be obtained by [Lemma 2.10](#). \square

4. Phased graph state and Gaussian elimination. In this section, we reveal the relation between phased graph states and Gaussian elimination. In [subsection 4.1](#), we define a generalized Gauss-Jordan elimination process for matrices in \mathbb{J}_n and show that the result of this process can be obtained by LDL decomposition over \mathbb{F}_2 . Also, we show that this process gives an amplitudes formula for Hadamard transformed phased graph states in [subsection 4.2](#).

4.1. A generalized Gauss-Jordan process. In this section, we define a generalized Gauss-Jordan elimination process for matrices in \mathbb{J}_n . For simplicity, we consider symmetric matrices with unpivoted LDL decompositions so that Gaussian elimination can be applied sequentially on the row/columns. Let \mathbb{W}_n be the subset of matrices in \mathbb{J}_n that admit an unpivoted LDL decomposition. More precisely,

$$(4.1) \quad \mathbb{W}_n = \{A \in \mathbb{J}_n \mid \omega_1(A) \text{ admits an LDL decomposition } (P, L, D) \text{ s.t. } P = I\}.$$

Note that any matrix in \mathbb{J}_n can be transformed to a matrix in \mathbb{W}_n by symmetric row/column permutation.

Consider a sequence of transformations (Gauss-Jordan process) based on eliminations of consecutive rows/columns or pairs of them for matrices in \mathbb{W}_n . This process is defined in [Algorithm 4.1](#), with the notation $a \leftarrow b$ meaning that the algorithm sets variable a to b . This process is designed to reflect the action of vertex and edge complementation on a graph state on an admissible sequence of distinct vertices. At the same time, with exception of the second bit of the diagonal, it is equivalent to Gauss-Jordan elimination (matrix inversion algorithm) over \mathbb{F}_2 .

LEMMA 4.1. *For any $A \in \mathbb{W}_n$, $k \in \mathbb{N}$, $k \leq \text{rank}(A)$, if $A_{11} \in \mathbb{W}_k$ is full rank, $[B, v] = \text{Gauss-Jordan-}\mathbb{W}_n(A, k)$ terminates successfully and satisfies the **Ensure** conditions in [Algorithm 4.1](#). In particular,*

$$(4.2) \quad \omega_1 \left(\begin{bmatrix} B_{11} & B_{12} \\ B_{21} & B_{22} \end{bmatrix} \right) = \omega_1 \left(\begin{bmatrix} A_{11}^\# & A_{11}^\# A_{12} \\ A_{21} A_{11}^\# & A_{22} - A_{21} A_{11}^\# A_{12} \end{bmatrix} \right),$$

additionally, using $\omega_1(A_{11}) = LDL^T \pmod{2}$,

$$(4.3) \quad B_{11} = \Omega_{1,2}(L^{-T}DL^{-1})$$

$$(4.4) \quad B_{22} = \Omega_{1,2}(A_{22} - A_{21}B_{11}A_{12})$$

$$(4.5) \quad v = d(\omega_2(LDL^T) \oplus \omega_2(A_{11})).$$

Proof. We refer to the ℓ 'th iteration of [Algorithm 4.1](#) as the **while** loop iteration when $i = \ell$. The requirement that $A_{11} \in \mathbb{W}_k$ is full rank, ensures that in the **else** clause, $\omega_1(\bar{A}_{11}) = \begin{bmatrix} 0 & 1 \\ 1 & 0 \end{bmatrix}$, and that the algorithm terminates with $i = k$. Further, note that in the Gauss-Jordan process for \mathbb{W}_n , the second bit of the diagonal of A or of B at any iteration ℓ has no effect on subsequent iterations in the process. Hence, modulo 2, the process is equivalent to Gauss-Jordan matrix inversion over \mathbb{F}_2 . It follows that [\(4.2\)](#) in the Lemma statement holds.

Algorithm 4.1 $[B, v] = \text{Gauss-Jordan-}\mathbb{W}_n(A, k)$

Require: $A \in \mathbb{W}_n$, $A_{11} \in \mathbb{W}_k$ is rank k .

Ensure: If $k < n$, with $A_{11} \in \mathbb{W}_k$,

$$B = \Gamma_k(A) = \Omega_{1,2} \left(\begin{bmatrix} \Gamma_k(A_{11}) & A_{11}^\# A_{12} \\ A_{21} A_{11}^\# & A_{22} - A_{21} \Gamma_k(A_{11}) A_{12} \end{bmatrix} \right).$$

While if $k = n$, for any $\ell \leq k$, with $A_{11} \in \mathbb{W}_\ell$,

$$B = \Omega_{1,2} \left(\begin{bmatrix} \Gamma_\ell(A_{11}) - B_{12} B_{22} B_{21} & B_{12} \\ B_{21} & B_{22} \end{bmatrix} \right),$$

$B_{12} = A_{11}^\# A_{12} B_{22}$, $B_{21} = B_{12}^T$, $B_{22} = \Gamma_{k-\ell}(A_{22} - A_{21} \Gamma_\ell(A_{11}) A_{12})$. Further, $v \in \mathbb{F}_2^k$ with $v_{\ell+1} = \omega_2(s_{11})$, where $S = A_{22} - A_{21} \Gamma_\ell(A_{11}) A_{12}$. Additionally if $\omega_1(s_{11}) = 0$, $v_{\ell+2} = \omega_2(s_{22})$.

1: $i \leftarrow 1$

2: $B \leftarrow A$

3: **while** $i < k$ **do**

4: $P \leftarrow \begin{bmatrix} 0 & I_{n-i+1} \\ I_{i-1} & 0 \end{bmatrix}$ where I_m is the $m \times m$ identity matrix

5: $\bar{A} \leftarrow P B P^T$.

6: **if** $\omega_1(\bar{a}_{11}) = 1$ **then**

7:

$$B \leftarrow P^T \Omega_{1,2} \left(\begin{bmatrix} \bar{a}_{11} & \bar{a}_{12} \\ \bar{a}_{21} & \bar{a}_{22} - \bar{a}_{21} \omega_1(\bar{a}_{11}) \bar{a}_{12} \end{bmatrix} \right) P.$$

8: $v_i \leftarrow \omega_2(b_{ii})$

9: $b_{ii} \leftarrow \omega_1(b_{ii})$

10: $i \leftarrow i + 1$

11: **else**

12: With $\bar{A}_{11} \in \mathbb{W}_2$, as

$$B \leftarrow P^T \Omega_{1,2} \left(\begin{bmatrix} \bar{A}_{11} & \omega_1(\bar{A}_{11}) \bar{A}_{12} \\ \bar{A}_{21} \omega_1(\bar{A}_{11}) & \bar{A}_{22} - \bar{A}_{21} \omega_1(\bar{A}_{11}) \bar{A}_{12} \end{bmatrix} \right) P,$$

13: $v_i \leftarrow \omega_2(b_{ii})$

14: $v_{i+1} \leftarrow \omega_2(b_{i+1,i+1})$

15: $b_{ii} \leftarrow \omega_1(b_{ii})$

16: $b_{i+1,i+1} \leftarrow \omega_1(b_{i+1,i+1})$

17: $i \leftarrow i + 2$

18: **end if**

19: **end while**

Further, to derive the form of v in (4.5), note that we may write the LDL decomposition as

$$LDL^T = \sum_{j=1}^t L_j D_j L_j^T,$$

where t is the number of diagonal blocks in D , and each L_j corresponds to one or two consecutive columns of L . Further, with A_{11} of the same dimensions as D_1 ,

$L_1 D_1 L_1^T = A_{21} \omega_1(A_{11}) A_{12} \pmod{2}$. Hence, after the first iteration in [Algorithm 4.1](#), we have $d(B) = d(A) - L_1 D_1 L_1^T$. The same holds for subsequent trailing matrix updates, except LDL does not update rows and columns that have already been eliminated. The vector v is defined accordingly, as v_ℓ is defined by the ℓ th value of the diagonal at iteration ℓ (just before it is eliminated). Hence, v is simply equal to the sum of the LDL trailing matrix updates with the original value of $\omega_2(d(A))$ and (4.5) in the Lemma holds.

Let

$$(4.6) \quad L = \begin{bmatrix} L_{11} & & \\ L_{21} & L_{22} & \\ L_{31} & L_{32} & L_{33} \end{bmatrix}$$

where $L_{11} \in \mathbb{F}_2^{\ell \times \ell}$ and $L_{22} \in \mathbb{F}_2^{s \times s}$ where $s = 1$ or $s = 2$ depending on the corresponding block of D . At the start of the ℓ th iteration of [Algorithm 4.1](#), we aim to show that we have

$$B = \begin{bmatrix} B_{11} & B_{12} & B_{12} \\ B_{21} & B_{22} & B_{23} \\ B_{31} & B_{32} & B_{33} \end{bmatrix}, B_{11} \in \mathbb{J}_\ell, B_{22} \in \mathbb{W}_s, B_{21} = \omega_1(L_{21} L_{11}^{-1}).$$

By equivalence to Gauss-Jordan inversion over \mathbb{F}_2 modulo 2, we have that

$$B_{21} = \omega_1(A_{21} A_{11}^\#) = \omega_1(L_{21} D_{11} L_{11}^T L_{11}^{-T} D_{11} L_{11}^{-1}) = \omega_1(L_{21} L_{11}^{-1}).$$

Hence, at the ℓ step, the update to the leading $\ell \times \ell$ block of B , B_{11} is

$$B_{11} \leftarrow \Omega_{1,2}(B_{11} - B_{12} \omega_1(B_{22}) B_{21}) = \Omega_{1,2}(B_{11} - L_{11}^{-T} L_{21}^T \omega_1(B_{22}) L_{21} L_{11}^{-1}).$$

Further, the off-diagonal block of L^{-1} is $\omega_1(L_{21} L_{11}^{-1})$ modulo 2 (the even part of L^{-1} does not contribute to $\Omega_{1,2}(L^{-T} D L^{-1})$). Hence, by induction, (4.3) holds.

It remains to show that trailing matrix updates result in a diagonal term as in (4.4), which also leads to the form of B asserted by the **Ensure** clause of [Algorithm 4.1](#). By the same argument as for v , using (4.3), we have that

$$(4.7) \quad B_{22} = \Omega_{1,2}(A_{22} - L_{21} D_{11} L_{12})$$

$$(4.8) \quad = \Omega_{1,2}(A_{22} - A_{21} L_{11}^{-T} D_{11} D_{11} D_{11} L_{11}^{-1} A_{12})$$

$$(4.9) \quad = \Omega_{1,2}(A_{22} - A_{21} B_{11} A_{12}). \quad \square$$

We now demonstrate how the \mathbb{W}_n Gauss-Jordan process corresponds to transformations of phased graph states. Let $\delta(A) = d(D)$ for $A \in \mathbb{W}_n$ and D being the block diagonal matrix in an LDL decomposition of A .

LEMMA 4.2. *For any $A \in \mathbb{W}_n$, $k \in \mathbb{N}$, $k \leq \text{rank}(A)$, if $A_{11} \in \mathbb{W}_k$ is full rank, $[B, v] = \text{Gauss-Jordan-}\mathbb{W}_n(A, k)$, let $B = \begin{bmatrix} B_{11} & B_{12} \\ B_{21} & B_{22} \end{bmatrix}$ where B_{11} is $k \times k$ and $u = v \oplus \delta(A_{11})$. Further, define $\bar{v} = \begin{bmatrix} v \\ 0 \end{bmatrix} \in \mathbb{F}_2^n$ and $\bar{u} = \begin{bmatrix} u \\ 0 \end{bmatrix} \in \mathbb{F}_2^n$. For any phased graph state $|A\rangle$,*

$$(H^{\otimes k} \otimes I^{\otimes(n-k)}) |A\rangle = \alpha X^{\bar{v}} Z^{\bar{u}} |B\rangle$$

for some $\alpha \in \mathbb{C}$.

Proof. We show that the two elimination cases in the Gauss-Jordan process ([Algorithm 4.1](#)) can be mapped to vertex and edge complementation, with a Hadamard gate acting on each eliminated row/column. We have that $|A\rangle = \hat{Z}^{d(A)} |O(A)\rangle$. Let

$$N = \Omega_{1,2} \left(\begin{bmatrix} a_{11} & a_{12} \\ a_{21} & A_{22} - a_{21}\omega_1(a_{11})a_{12} \end{bmatrix} \right).$$

Let $\bar{a}_{21} = \begin{bmatrix} 0 \\ a_{21} \end{bmatrix}$. By [Theorem 2.6](#), vertex complementation on the first vertex in $|O(A)\rangle$ gives,

$$(4.10) \quad |O(A)\rangle = \check{X}^{(1)} \prod_{i \in \{2, \dots, n\}, a_{1i} \neq 0} \hat{Z}^{(i)} |O(N)\rangle$$

$$(4.11) \quad = \check{X}^{(1)} \hat{Z}^{\bar{a}_{21}} |O(N)\rangle.$$

We can express the Hadamard gate as $H = \frac{1+i}{\sqrt{2}} \check{X} \hat{Z} \check{X}$, so $\check{X} = \frac{\sqrt{2}}{1+i} H \hat{X} \hat{Z}$, and

$$(4.12) \quad |O(A)\rangle = \frac{\sqrt{2}}{1+i} H^{(1)} \hat{X}^{(1)} \hat{Z}^{(1)} \hat{Z}^{\bar{a}_{21}} |O(N)\rangle.$$

Hence,

$$(4.13) \quad H^{(1)} |A\rangle = H^{(1)} \check{Z}^{d(A)} |O(A)\rangle$$

$$(4.14) \quad = (\check{X}^{a_{11}})^{(1)} H^{(1)} \check{Z}^{d(A) - e_1 a_{11}} |O(A)\rangle$$

$$(4.15) \quad = \frac{\sqrt{2}}{1+i} (\check{X}^{a_{11}})^{(1)} H^{(1)} \check{Z}^{d(A) - e_1 a_{11}} H^{(1)} \hat{X}^{(1)} \hat{Z}^{(1)} \hat{Z}^{\bar{a}_{21}} |O(N)\rangle$$

$$(4.16) \quad = \frac{\sqrt{2}}{1+i} (X^{\omega_2(a_{11})})^{(1)} \check{Z}^{d(A) - e_1 a_{11}} \hat{Z}^{(1)} \hat{Z}^{\bar{a}_{21}} |O(N)\rangle$$

$$(4.17) \quad = \frac{\sqrt{2}}{1+i} (X^{\omega_2(a_{11})} Z^{\omega_2(a_{11})})^{(1)} \check{Z}^{d(A)} Z^{(1)} \hat{Z}^{\bar{a}_{21}} |O(N)\rangle$$

$$(4.18) \quad = \frac{\sqrt{2}}{1+i} (X^{\omega_2(a_{11})} Z^{\omega_2(a_{11})+1})^{(1)} |N\rangle.$$

The term $\omega_2(a_{11})$ is exactly the definition of v_i modulo the permutation performed in the Gauss-Jordan process. The additional $Z^{(1)}$ is as needed since $\delta(A)_i = 1$.

In the case of edge complementation, let

$$M = \Omega_{1,2} \left(\begin{bmatrix} A_{11} & A_{11}A_{12} \\ A_{21}A_{11} & A_{22} - A_{21}\omega_1(A_{11})A_{12} \end{bmatrix} \right).$$

By [Theorem 2.7](#), we have

$$(4.19) \quad |O(A)\rangle = H^{(1)} H^{(2)} Z^{a_1 * a_2} |O(M)\rangle,$$

where $*$ is the Hadamard (elementwise) product. Further,

$$(4.20) \quad H^{(1)} H^{(2)} |A\rangle = H^{(1)} H^{(2)} \check{Z}^{d(A)} |O(A)\rangle$$

$$(4.21) \quad = (X^{\omega_2(a_{11})})^{(1)} (X^{\omega_2(a_{22})})^{(2)} H^{(1)} H^{(2)} \check{Z}^{d(A) - e_1 a_{11} - e_2 a_{22}} |O(A)\rangle$$

$$(4.22) \quad = (X^{\omega_2(a_{11})} Z^{\omega_2(a_{11})})^{(1)} (X^{\omega_2(a_{22})} Z^{\omega_2(a_{22})})^{(2)} \check{Z}^{d(A) - 2a_1 * a_2} |O(M)\rangle$$

$$(4.23) \quad = (X^{\omega_2(a_{11})} Z^{\omega_2(a_{11})})^{(1)} (X^{\omega_2(a_{22})} Z^{\omega_2(a_{22})})^{(2)} |M\rangle.$$

Applying the above inductively leads to the equivalence stated in the lemma with $\alpha = (\sqrt{2}/(1+i))^{\sum_j v_j}$. \square

4.2. An amplitude formula for Hadamard-transformed phased graph states. A direct formula for the amplitudes of $H^{\otimes n} |A\rangle$ is given by [Theorem 4.5](#) if $\omega_1(A)$ is full rank over \mathbb{F}_2 , via an n -step \mathbb{W}_n Gauss-Jordan process. We now consider the general case, with $\text{rank}(\omega_1(A)) = k$. To obtain this formula, we need to work out the action of the remaining $n - k$ Hadamard gates acting on the trailing $n - k$ qubits of $|A\rangle$. The following well-known lemma describes the action of $n - k$ Hadamard gates on a general state.

LEMMA 4.3. *Let $x_1 \in \mathbb{F}_2^k$, $x_2 \in \mathbb{F}_2^{n-k}$, and $|\psi\rangle$ be an n -qubit quantum state. Then*

$$(4.24) \quad \left\langle \begin{bmatrix} x_1 \\ x_2 \end{bmatrix} \middle| I^{\otimes k} \otimes H^{\otimes(n-k)} \middle| \psi \right\rangle = 2^{-(n-k)/2} \sum_{y_2 \in \mathbb{F}_2^{(n-k)}} (-1)^{y_2^T x_2} \left\langle \begin{bmatrix} x_1 \\ y_2 \end{bmatrix} \middle| \psi \right\rangle.$$

Proof. For $x, y \in \mathbb{F}_2$, we have $\langle x | H | y \rangle = (-1)^{xy}$. Then the lemma follows. \square

We leverage the fact that $\omega_1(A^{(k)})$ has a block saddle point structure (the Schur complement of $\omega_1(A_{11}) \in \mathbb{F}_2^{k \times k}$ must be zero if the rank of $\omega_1(A)$ is k).

LEMMA 4.4. *Consider any $B \in \mathbb{J}_n$ such that*

$$B = \begin{bmatrix} B_{11} & B_{12} \\ B_{21} & B_{22} \end{bmatrix}, \quad B_{11} \in \mathbb{J}_k, \quad \omega_1(B_{22}) = 0.$$

Then for all $x_1 \in \mathbb{F}_2^k$, $x_2 \in \mathbb{F}_2^{n-k}$,

$$\left\langle \begin{bmatrix} x_1 \\ x_2 \end{bmatrix} \middle| I^{\otimes k} \otimes H^{\otimes(n-k)} \middle| B \right\rangle = \begin{cases} 2^{-k/2} i^{-x_1^T B_{11} x_1} & x_2 = \omega_1(B_{21} x_1 + z) \\ 0 & \text{otherwise.} \end{cases}$$

where $z = \omega_2(d(B_{22}))$.

Proof. By [Definition 3.1](#) and the specified structure of B , we have

$$(4.25) \quad \langle x | A \rangle = 2^{-n/2} i^{-x_1^T B_{11} x_1} (-1)^{x_2^T (B_{21} x_1 + z)}$$

Then applying [Lemma 4.3](#), we get

$$(4.26) \quad \left\langle \begin{bmatrix} x_1 \\ x_2 \end{bmatrix} \middle| I^{\otimes k} \otimes H^{\otimes(n-k)} \middle| B \right\rangle$$

$$(4.27) \quad = 2^{-(2n-k)/2} i^{-x_1^T B_{11} x_1} \sum_{y_2 \in \mathbb{F}_2^{(n-k)}} (-1)^{y_2^T (B_{21} x_1 + x_2 + z)}$$

$$(4.28) \quad = \begin{cases} 2^{-k/2} i^{-x_1^T B_{11} x_1} & x_2 = \omega_1(B_{21} x_1 + z) \\ 0 & \text{otherwise.} \end{cases}$$

This completes the proof. \square

To obtain the full formula for $\langle x | H^{\otimes n} |A\rangle$, it suffices to combine [Lemma 4.2](#) and [Lemma 4.4](#).

THEOREM 4.5. *Given $A \in \mathbb{W}_n$ where $\text{rank}(\omega_1(A)) = k$ and v, u, B defined as in [Lemma 4.2](#). Let B_{11} and B_{22} be diagonal blocks of B such that $B_{11} \in \mathbb{J}_k$ and $B_{22} \in \mathbb{J}_{n-k}$. Let $w = \begin{bmatrix} v \\ \omega_2(d(B_{22})) \end{bmatrix}$. Then for any $x \in \mathbb{F}_2^n$,*

$$(4.29) \quad \langle x | H^{\otimes n} |A\rangle = \begin{cases} 2^{-k/2} i^{-(x_1+v)^T (B_{11}+2D(u))(x_1+v)} & x \oplus w \in \text{span}(\omega_1(A)) \\ 0 & \text{otherwise} \end{cases}$$

where x_1 are the leading k elements of x .

Proof. Let x_2 , v_2 and u_2 denote the trailing $n - k$ elements of x , v and u respectively. By [Lemma 4.2](#),

$$(4.30) \quad \langle x | H^{\otimes n} | A \rangle = \langle x | (I^{\otimes k} \otimes H^{\otimes(n-k)})(H^{\otimes k} \otimes I^{\otimes(n-k)}) | A \rangle$$

$$(4.31) \quad = \langle x | (I^{\otimes k} \otimes H^{\otimes(n-k)}) X^v Z^u | B \rangle$$

$$(4.32) \quad = \langle x | X^v Z^u (I^{\otimes k} \otimes H^{\otimes(n-k)}) | B \rangle$$

$$(4.33) \quad = \langle \omega_1(x + v) | Z^u (I^{\otimes k} \otimes H^{\otimes(n-k)}) | B \rangle$$

$$(4.34) \quad = (-1)^{(x_1+v)^T u} \langle \omega_1(x + v) | I^{\otimes k} \otimes H^{\otimes(n-k)} | B \rangle.$$

Let $z = \omega_2(d(B_{22}))$. By [Lemma 4.4](#), we have the following when $x_2 = \omega_1(B_{21}(x_1 + v) + z)$,

$$(4.35) \quad \langle x | H^{\otimes n} | A \rangle = 2^{-k/2} j^{-\omega_1(x_1+v)^T B_{11} \omega_1(x_1+v) - 2(x_1+v)^T u}$$

$$(4.36) \quad = 2^{-k/2} j^{-(x_1+v)^T B_{11}(x_1+v) - 2(x_1+v)^T u}$$

$$(4.37) \quad = 2^{-k/2} j^{-(x_1+v)^T (B_{11} + 2D(u))(x_1+v)}$$

Also, if $x_2 \neq \omega_1(B_{21}(x_1 + v) + z)$,

$$\langle x | H^{\otimes n} | A \rangle = 0.$$

Finally, we show the condition $x_2 = \omega_1(B_{21}(x_1 + v) + z)$ is equivalent to $x \oplus w \in \text{span}(A)$. When the condition is satisfied, we have

$$(4.38) \quad \begin{bmatrix} B_{11} & B_{12} \\ B_{21} & 0 \end{bmatrix} \begin{bmatrix} x_1 + v \\ 0 \end{bmatrix} \equiv \begin{bmatrix} B_{11}(x_1 + v) \\ x_2 + z \end{bmatrix} \pmod{2}.$$

And further, by the domain-range exchange property of principal pivot transform [\[35, Theorem 3.1\]](#), the above implies that

$$(4.39) \quad \begin{bmatrix} A_{11} & A_{12} \\ A_{21} & A_{22} \end{bmatrix} \begin{bmatrix} B_{11}(x_1 + v) \\ 0 \end{bmatrix} \equiv \begin{bmatrix} x_1 + v \\ x_2 + z \end{bmatrix} \pmod{2}.$$

Hence, the right-hand side above, $x \oplus w$, must be in the span of $\omega_1(A)$ over \mathbb{F}_2 . Further, if $x \oplus w \in \text{span}(\omega_1(A))$, the above condition must hold, since the first k columns of A have the same span as all of the columns of A . \square

5. Phased graph state simulation. In this section, we utilize the relation between phased graph states and Gaussian elimination as presented in [section 4](#) with techniques in numerical linear algebra to solve the phased graph state simulation problem as defined in [Definition 3.3](#).

5.1. Usage of implicit fast LDL decomposition. As shown in [Lemma 4.1](#), the generalized Gauss-Jordan process is closely related to LDL decompositions. Therefore, the fast LDL algorithm [\[32\]](#) can be applied here to solve the phased graph state simulation problem in running time depending on the treewidth of the graph. However, extra caution is needed because the fast LDL algorithm represents the decomposition in an implicit form and we need to make sure all of the intermediate steps for phased graph state simulation can be performed efficiently. We first provide a lemma that computes parts of the inverse based on a sparse LDL decomposition, then show how to use it to compute all non-trivial quantities needed later from L .

LEMMA 5.1. Consider a symmetric matrix $A \in \mathbb{F}_2^{n \times n}$ with a tree decomposition $T = (V_T, E_T)$ of width τ with $O(n/\tau)$ bags corresponding to a rooted binary tree. Let P be the permutation obtained from the LDL algorithm in [32]. Let A_{11} be the maximal leading square full-rank block of $P^T A P$, and consider

$$(P^T A P)^g = \begin{bmatrix} A_{11}^\# & A_{11}^\# A_{12} \\ A_{21} A_{11}^\# & 0 \end{bmatrix}$$

Let $X_B = P_B^T X P_B$ be the restriction of X to the vertices of a bag B of the tree decomposition (each column of P_B is a distinct elementary vector) for any $X \in \mathbb{F}_2^{n \times n}$. The set of matrices $\{(P(P^T A P)^g P)_B | B \in V_T\}$ may be computed in time $O(n\tau^{\omega-1})$.

Proof. We can compute these blocks by induction, starting from the root node of the tree decomposition. For the root node bag R , it suffices to directly compute A_R^g from the Schur complement (which may be formed from the lower right block of the triangular part of the L factor and the corresponding part of D). For any non-root bag B , we assume that we have access to A_P^g where P is the parent of B . Compute A_P^h by zeroing out all rows/columns of A_P^g corresponding to peeled rows/columns (not part of the leading full rank block), and removing all rows/columns that are not in B . Define \bar{A}_P^h by setting the diagonal entries corresponding to zero rows/columns, to 1. Now, let $K \subseteq B$ the set of vertices in B not contained in P and let M be the remaining vertices in B . Assume $Y = A_B^g$ is ordered so that vertices in K appear after vertices in M . We may obtain the leading $|M|$ -dimensional block of Y , Y_{11} directly from A_P^g . To get Y_{21} and Y_{22} , we may use products like $A_{KM} A_P^h A_{MK}$ where A_{KM} is the off-diagonal block of A between vertices in K and vertices in M . In particular, for a 2-node tree with nodes B and P , we have that the initial A has the block structure,

$$A = \begin{bmatrix} A_{11} & A_{12} & 0 \\ A_{21} & A_{22} & A_{23} \\ 0 & A_{32} & A_{33} \end{bmatrix}, \quad A_{11} \in \mathbb{F}_2^{|K| \times |K|}, A_{22} \in \mathbb{F}_2^{|M| \times |M|}.$$

Let $B = A_P^h$ and $\bar{B} = \bar{A}_P^h$, where we have (in this case), $A_P = \begin{bmatrix} A_{22} & A_{23} \\ A_{32} & A_{33} \end{bmatrix}$. Define A_{11}^h and \bar{A}_{11}^h analogously to A_P^h and \bar{A}_P^h . Then, we have that

$$P(P^T A P)^g P = \begin{bmatrix} A_{11}^g - \bar{A}_{11}^h A_{12} B A_{21} \bar{A}_{11}^h & \bar{A}_{11}^h A_{12} \bar{B}_{11} & * \\ \bar{B}_{11} A_{21} \bar{A}_{11}^h & (A_P^g)_{11} & (A_P^g)_{12} \\ * & (A_P^g)_{21} & (A_P^g)_{22} \end{bmatrix},$$

where $*$ denotes blocks we are not interested in computing. Clearly, the block matrix multiplications we are interested in computing have dimension smaller than the bag size. When there are more than 2 nodes, in particular when B has descendants, the situation does not change, except that we should start with the Schur complement obtained after eliminating all descendants of B instead of simply A . Hence, it suffices to do $O(\tau^\omega)$ work for each of $O(n/\tau)$ nodes, leading to the complexity in the lemma. \square

An alternate algorithm (proof of the above lemma) is to compute an LDL decomposition for every bag in the tree decomposition, with that bag as root. For each LDL the desired block of the inverse is trivial to obtain from the root node. The $O(n/\tau)$ LDL decompositions can be computed in $O(\tau^\omega)$ amortized time each, by shifting the root following an Euler tour of the tree, and recomputing the LDL for only $O(1)$ bags at each step in the tour.

Leveraging the sparse LDL and partial inverse construction algorithms, we provide the following lemma to summarize the complexities of subroutines that are needed for phased graph state simulation based on the fast LDL algorithm described in [32].

LEMMA 5.2. *Given $A \in \mathbb{W}_n$ such that $\text{rank}(\omega_1(A)) = k$ and a tree decomposition of the graph corresponding to A with width τ , then the fast LDL algorithm [32] can compute an implicit representation of $L \in \mathbb{F}_2^{n \times k}$ and $D \in \mathbb{F}_2^{k \times k}$ in $O(n\tau^{\omega-1})$ time, such that the following conditions are all satisfied,*

- $\omega_1(A) = \omega_1(LDL^T)$ is a reduced LDL decomposition over \mathbb{F}_2 .
- Let $L = \begin{bmatrix} L_1 \\ L_2 \end{bmatrix}$ where $L_1 \in \mathbb{F}_2^{k \times k}$. Then the matrix-vector product with L_1 , L_1^{-1} or $L_2L_1^{-1}$ over \mathbb{F}_2 could be performed in $O(n\tau)$ time.
- Let $\tilde{L} = \begin{bmatrix} L_1 & 0 \\ L_2 & I \end{bmatrix}$ for L_1, L_2 as defined above. Then for any $X \in \mathbb{F}_2^{n \times \tau}$, $\tilde{L}X$, $\tilde{L}^T X$, $\tilde{L}^{-1}X$, or $\tilde{L}^{-T}X$ over \mathbb{F}_2 could be computed in $O(n\tau^{\omega-1})$ time.

Moreover, $\omega_2(d(L_1^{-T}DL_1^{-1}))$ as well as v and w as defined in Theorem 4.5 can be computed along with the LDL decomposition without increasing the time complexity.

Proof. The fast LDL algorithm described in [32] takes $O(n\tau^{\omega-1})$ time and represents $L = \omega_1(\prod_i^m Q_i)$ for $m = O(n/\tau)$ such that each Q_i acts on a submatrix of size $O(\tau)$. Therefore, the three conditions in the lemma are satisfied. For computing v (recall that v_i corresponds to the second bit of the diagonal in the Gauss-Jordan process when it is eliminated), it suffices to keep track of (but not propagate/use) the second bit of Schur complement updates to the diagonal. Its easy to check that computing this does not change the complexity of the LDL (no greater asymptotic number of operations over \mathbb{F}_2 required, even when considering fast matrix multiplication).

However, obtaining the second part of w (recall that it is defined to be $\omega_2(d(B_{22}))$) for B_{22} as given in Lemma 4.1 that corresponds to nodes that are not eliminated in the Gauss-Jordan process) is trickier with the sparse LDL procedure in [32], because linearly-dependent rows are peeled-off early in the factorization and we do not have the corresponding rows of L explicitly. To overcome this without an efficient algorithm for explicit construction of the rows of L , we may leverage Lemma 5.1, which gives an explicit formula for computing the generalized inverse based on the Gauss-Jordan process for all diagonal blocks. To obtain w , it suffices to keep track of the second bit of the diagonal in the products in that formula (also when computing the Schur complement itself). The term $\omega_2(d(L_1^{-T}DL_1^{-1}))$ can be similarly computed via keeping track of the second bit of the diagonal in the recursive procedure of Lemma 5.1, but this time not combining it with the regular LDL updates to the Schur complement (updates from eliminations of descendant of descendants of bag B in the proof of Lemma 5.1). \square

5.2. Weak simulation of phased graph states. Since the nonzero amplitudes of a phased graph state have equal magnitude as given in Theorem 4.5, we are interested in uniform sampling of

$$(5.1) \quad \{x \in \mathcal{X}_{S,y} \mid x \oplus w \in \text{span}(\omega_1(A))\}.$$

We can assume, WLOG, that $w = 0$, since if $w \neq 0$ it suffices to produce the sample $x \oplus w$ then subtract w modulo 2. Hence, we focus on sampling

$$(5.2) \quad \mathcal{Y}_{A,S,y} = \{x \in \mathcal{X}_{S,y} \mid x \in \text{span}(\omega_1(A))\}.$$

Further, given the decomposition, $\omega_1(A) = LDL^T$ with trapezoidal L , since L preserves the span of $\omega_1(A)$,

$$\mathcal{Y}_{A,S,y} = \mathcal{Y}_{L,S,y}.$$

For vector spaces V and W , let $\text{span}(V) \setminus \text{span}(W)$ denote the quotient space defined by the intersecting subspace,

$$(5.3) \quad \text{span}(V) \setminus \text{span}(W) = \text{span}(V) / (\text{span}(V) \cap \text{span}(W)).$$

Then we have the following lemma that decomposes $\mathcal{Y}_{A,S,y}$.

LEMMA 5.3. *For any lower-trapezoidal, unit-diagonal matrix $L \in \mathbb{F}_2^{n \times r}$, any set $\bar{S} = \{\bar{s}_1, \dots, \bar{s}_\ell\} \subseteq \{1, \dots, n\}$, and vector $y \in \mathbb{F}_2^n$, such that $\forall i \in \bar{S}, y_i = 0$. Let*

$$\bar{B} = [e_{\bar{s}_1} \quad \dots \quad e_{\bar{s}_\ell}],$$

then, we have that either $\mathcal{Y}_{L,S,y} = \emptyset$ or

$$(5.4) \quad \exists x^\perp \in \text{span}(\bar{B}) \setminus \text{span}(L), x^\perp \in \text{span}(L), \text{ s.t. } x^\perp \oplus x^\perp = y \text{ and}$$

$$(5.5) \quad \forall x \in \mathcal{Y}_{L,S,y}, x = u(x) \oplus y \oplus x^\perp, u(x) \in \text{span}(\bar{B}) \cap \text{span}(L).$$

Moreover, if $L_1 \in \mathbb{F}_2^{r \times r}$ is the leading triangular block of L and $y_1 \in \mathbb{F}_2^r$ is the first r elements of y ,

$$(5.6) \quad x^\perp = \omega_1 \left(\begin{bmatrix} y_1 \\ L_2 L_1^{-1} y_1 \end{bmatrix} \right).$$

Proof. If $\mathcal{Y}_{L,S,y} \neq \emptyset$, there must exist a unique vector

$$x^\perp \in \text{span}(\bar{B}) \setminus \text{span}(L),$$

such that $x^\perp = y \oplus x^\perp \in \text{span}(L)$, i.e.,

$$(5.7) \quad \mathcal{Y}_{L,S,y} = \{x \mid x = x^\perp \oplus y, x^\perp \in \text{span}(\bar{B}) \setminus \text{span}(L), x \in \text{span}(L)\},$$

and hence (5.4) holds. Further, (5.5) follows, as for any $v, w \in \mathcal{Y}_{L,S,y}$, we must have $v \oplus w \in \text{span}(L) \cap \text{span}(\bar{B})$ since $\text{span}(\bar{B})$ includes all vectors in $\mathcal{X}_{S,0}$. Further, the projection matrix on $\text{span}(L)$ is,

$$P = \begin{bmatrix} L_1 \\ L_2 \end{bmatrix} \begin{bmatrix} L_1^{-1} & 0 \end{bmatrix} = \begin{bmatrix} I & 0 \\ L_2 L_1^{-1} & 0 \end{bmatrix} \pmod{2}.$$

We can verify that it is the projector because $P^2 = P$, $\text{span}(P) = \text{span}(L)$. Then, $x^\perp = Py$ gives (5.6). \square

Given that Lemma 5.3 gives a way to obtain x^\perp by triangular solve, we may subsequently just compute $x^\perp = y \oplus x^\perp$ and check if $x^\perp \in \text{span}(B) \Leftrightarrow x^\perp \in \mathcal{X}_{S,0}$ to determine whether $\mathcal{Y}_{L,S,y} = \emptyset$.

It then remains to devise a routine to sample $u(x)$, i.e., uniformly sample $\text{span}(L) \cap \text{span}(B)$. Note that we can compute the intersection of vector space by finding the quotient of the null space of B ,

$$(5.8) \quad \text{span}(L) \cap \text{span}(\bar{B}) = \text{span}(L) \setminus \text{span}(B), B = [e_{s_1} \quad \dots \quad e_{s_{n-\ell}}].$$

Further,

$$(5.9) \quad \text{span}(L) \cap \text{span}(\bar{B}) = \text{span} \left(P^T \begin{bmatrix} 0 \\ \hat{L}_2 \end{bmatrix} \right), \quad \hat{L} = PL, \quad PB = \begin{bmatrix} I \\ 0 \end{bmatrix},$$

where P is a permutation matrix and \hat{L}_2 is the lower $\ell \times r$ block of \hat{L} . Hence, we can sample $u(x)$ by finding a random linear combination of linearly independent columns of \hat{L}_2 . Due to the trapezoidal structure of L , it would suffice to omit some rows and columns of L to get a basis for this subspace. In particular, let $M \in \mathbb{F}_2^{n \times n}$ be the diagonal matrix that zeros out the $(n-l)$ rows of L specified in (5.9), i.e. $m_{jj} = 1$ iff $e_j \in \text{span}(\bar{B})$. Also, let $N \in \mathbb{F}_2^{n \times n}$ be the diagonal matrix that zeros out the linearly dependent columns of L , i.e. the columns corresponding to the leading r rows of L that are zeroed out by M . Alternatively, N can be defined as the leading $r \times r$ diagonal block of M . Then $u(x)$ can be sampled by computing $MLNc$ for uniformly random $c \in \mathbb{F}_2^r$.

The complexity of the sampling algorithm described above is given in the following theorem.

THEOREM 5.4 (Complexity of weak phased graph state simulation). *Given any $y \in \mathbb{F}_2^n$, $S \subseteq [n]$, $A \in \mathbb{J}_n$ and a tree decomposition of the graph corresponding to A with width τ , uniformly sampling $k \in \mathbb{N}$ elements from*

$$\{x \in \mathcal{X}_{S,y} \mid x \oplus w \in \text{span}(\omega_1(A))\},$$

where w is defined as in [Theorem 4.5](#), or reporting the set is empty, could be done in $O(n\tau^{\omega-1} + \min(kn\tau^{\omega-2}, \ell n\tau^{\omega-2} + k\ell^{\omega-1}))$ time for $\ell = n - |S|$.

Proof. Assume, WLOG, $A \in \mathbb{W}_n$. By [Lemma 5.2](#), we can compute an implicit LDL decomposition of $\omega_1(A)$ as well as the vector w in $O(n\tau^{\omega-1})$ time.

The first step is to check whether the set we seek to sample is empty. By [Lemma 5.3](#), x^\perp can be computed by applying $L_2L_1^{-1}$, which takes $O(n\tau^{\omega-1})$ time according to [Lemma 5.2](#). Then we need to check $y \oplus x^\perp \in \text{span}(B) \iff \mathcal{Y}_{L,S,y} = \emptyset$. This is also in $O(n\tau^{\omega-1})$ time with the implicit LDL given by [Lemma 5.2](#).

Then we sample $u(x)$ by computing $MLNc$ for uniformly random $c \in \mathbb{F}_2^r$. By [Lemma 5.2](#), performing this matrix-vector product with the implicit form of L takes $O(n\tau)$ time, and to sample k times, the multiplication could be done in k/τ batches in $O(kn\tau^{\omega-2})$ time.

However, if ℓ is relatively small (i.e. $\ell < n\tau$), it is preferable to explicitly form the basis of the subspace. Note that N contains at most ℓ nonzero columns, so MLN could be computed in $O(\ell n\tau^{\omega-2})$ time with ℓ/τ batches of matrix-matrix multiplication with the implicit L given by [Lemma 5.2](#). After that, sampling for k times could be done by k/ℓ batches of fast matrix multiplication, which takes $O(k\ell^{\omega-1})$ time. \square

5.3. Strong simulation of phased graph states. The strong simulation of phased graph state simulation boils down to the evaluation of the amplitudes formula in [Theorem 4.5](#), which could be evaluated in the same cost of fast LDL decomposition.

THEOREM 5.5 (Complexity of strong phased graph state simulation). *Given k binary strings $x^{(1)}, \dots, x^{(k)} \in \mathbb{F}_2^n$, $A \in \mathbb{J}_n$ and a tree decomposition of the graph corresponding to A with width τ , the amplitudes formula (4.29) in [Theorem 4.5](#) can be evaluated for all $x = x^{(1)}, \dots, x^{(k)}$ in $O(n\tau^{\omega-1} + kn\tau^{\omega-2})$ time.*

Proof. Assume WLOG that $A \in \mathbb{W}_n$. By [Lemma 5.2](#), we can compute an implicit LDL decomposition of $\omega_1(A)$ as well as the vector v and w as defined in [Theorem 4.5](#) in

$O(n\tau^{\omega-1})$ time. Then we check the complexity of evaluating (4.29), which is restated below,

$$(5.10) \quad \langle x | H^{\otimes n} | A \rangle = \begin{cases} 2^{-k/2} i^{-(x_1+v)^T (B_{11}+2D(u))(x_1+v)} & x \oplus w \in \text{span}(\omega_1(A)) \\ 0 & \text{otherwise.} \end{cases}$$

Then $x \oplus w \in \text{span}(\omega_1(A))$ could be checked by solving the systems $Ly = x \oplus w$ for $x = x^{(1)}, \dots, x^{(k)}$. This can be done in $O(kn\tau^{\omega-2})$ time using k/τ batches of fast matrix multiplications by Lemma 5.2. Further, since $u = v \oplus d(D)$, it remains to compute $x_1^T B_{11} x_1$ in the amplitudes formula (5.10) for all $x = x^{(1)}, \dots, x^{(k)}$. Note that

$$(5.11) \quad x_1^T B_{11} x_1 = x_1^T \Omega_{1,2} (L_1^{-T} D L_1^{-1}) x_1$$

$$(5.12) \quad = x_1^T \omega_1 (L_1^{-T} D L_1^{-1}) x_1 + 2x_1^T d(\omega_2 (L_1^{-T} D L_1^{-1})).$$

Since $d(\omega_2 (L_1^{-T} D L_1^{-1}))$ can be computed along with the LDL, the remaining cost is dominated by the first term, which can also be computed in $O(kn\tau^{\omega-2})$ time using k/τ batches of fast matrix multiplications by Lemma 5.2. \square

In applications such as circuit simulation, the x 's for which to compute amplitudes often share common parts. In this case, it can be more efficient to precompute the part of the amplitudes formula corresponding the shared parts of x to avoid repetitive work in a similar way as in weak simulation. This is detailed in the following theorem.

THEOREM 5.6. *Given k binary strings $x^{(1)}, \dots, x^{(k)} \in \mathcal{X}_{S,y}$ for some $S \subseteq [n]$ and $y \in \mathbb{F}_2^n$ such that $y_i = 0$ for $i \notin S$, $A \in \mathbb{J}_n$ and a tree decomposition of the graph corresponding to A with width τ , the amplitudes formula (4.29) in Theorem 4.5 can be evaluated for all $x = x^{(1)}, \dots, x^{(k)}$ in $O(n\tau^{\omega-1} + \ell n\tau^{\omega-2} + k\ell^{\omega-1})$ time for $\ell = n - |S|$.*

Proof. To check the zero condition of (4.29), we follow the weak simulation algorithm in subsection 5.2. Firstly, we compute an implicit reduced LDL decomposition of $\omega_1(A)$ as well as w, u, v as defined in Theorem 4.5. Then we can check $\mathcal{Y}_{L,S,y} = \emptyset$ in the same way as in weak simulation. If so, we return zeros for all amplitudes. Otherwise, we can explicitly form the basis of $\text{span}(L) \cap \text{span}(\bar{B})$. This step takes $O(n\tau^{\omega-1} + \ell n\tau^{\omega-2})$ time with the same analysis for weak simulation as in the proof of Theorem 5.4 based on the implicit LDL given by Lemma 5.2.

By Lemma 5.3, we can check $x \oplus w \oplus y \oplus x^\perp \in \text{span}(L) \cap \text{span}(\bar{B}) \iff \langle x | H^{\otimes n} | A \rangle = 0$ for $x = x^{(1)}, \dots, x^{(k)}$. This can be done by k/ℓ batches of fast matrix multiplication using the explicit basis computed in the previous step in $O(k\ell^{\omega-1})$ time. It then remains to compute the exponent in the amplitude formula (4.29). This can be done by evaluating (5.12) in Theorem 5.5, except that at most ℓ elements of x_1 varies for all $x_1 = x_1^{(1)}, \dots, x_1^{(k)}$. Therefore, the computation is dominated by multiplications of $\ell \times \ell$ matrices and takes $O(k\ell^{\omega-1})$ time with batches of fast matrix multiplication. \square

6. Applications in simulation. In this section, we apply our results to several simulation problems. In subsection 6.1, we show that our algorithm solves the graph state simulation problem and matches the complexity of the state of art [20]. Then we apply our algorithm to Clifford circuit simulation in subsection 6.2 and Clifford+T circuit simulation in subsection 6.3 and compare the complexities with known techniques.

6.1. Graph state simulation. The graph state simulation problem [20] is of independent interest due to the wide application of graph states, which is defined as follows.

DEFINITION 6.1 (Graph state simulation [20, 24]). *Let $G = (V, E)$ be a simple graph and each vertex $i \in V$ is associated with a unitary $U_i \in \{H, H\check{Z}, I\}$. Let $U_{base} = \bigotimes_{i \in V} U_i$. The strong simulation of G takes any $x \in \mathbb{F}_2^{|V|}$ as input, and outputs*

$$\langle x | U_{base} | G \rangle.$$

The weak simulation takes $S \subseteq V$ and $y \in \mathbb{F}_2^S$ as input, and samples $x \in \mathcal{X}_{S,y}$ from the distribution,

$$p(x) \propto |\langle x | U_{base} | G \rangle|^2.$$

Note that applying H , $H\check{Z}$, or I gate to a state and then measuring it in computational basis can be viewed as measuring the state in Pauli X, Y or Z basis respectively.

We claim that phased graph state simulation problem as defined in Definition 3.3 is equivalent to Definition 6.1 because all vertices measured in Z basis can be trimmed in linear time using the following property of graph states [31].

LEMMA 6.2. *Let $G = (V, E)$ be a graph, $v \in V$ and $b \in \mathbb{F}_2$. Then*

$$\langle b |^{(v)} | G \rangle = \frac{1}{\sqrt{2}} \prod_{u \in N(v)} \left(Z^{(u)} \right)^b | G \setminus \{v\} \rangle.$$

Proof. Assume WLOG that v is the first vertex in G . Then by definition,

$$\begin{aligned} |G\rangle &= \prod_{ij \in E} U_{CZ}^{(i,j)} |+\rangle^{\otimes |V|} \\ &= \prod_{u \in N(v)} U_{CZ}^{(u,v)} \prod_{ij \in E, i \neq v, j \neq v} U_{CZ}^{(i,j)} |+\rangle^{\otimes |V|} \\ &= \prod_{u \in N(v)} U_{CZ}^{(u,v)} |+\rangle \otimes |G \setminus \{v\}\rangle, \end{aligned}$$

since $U_{CZ}^{(i,j)}$ commutes with each other. Note that $|+\rangle = \frac{1}{\sqrt{2}}(|0\rangle + |1\rangle)$, and U_{CZ} does nothing if the first qubit is $|0\rangle$ and applies Z to the second qubit if the first qubit is $|1\rangle$. So, the equation above can be written as

$$|G\rangle = \frac{1}{\sqrt{2}} |0\rangle \otimes |G \setminus \{v\}\rangle + \frac{1}{\sqrt{2}} \prod_{u \in N(v)} Z^{(u)} |1\rangle \otimes |G \setminus \{v\}\rangle.$$

Applying $\langle b |^{(v)}$ to this equation completes the proof. \square

Then we have the following theorem that matches the $O(n\tau^{\omega-1})$ time complexity of single-sample weak graph state simulation in [20] and improve the the $O(n\tau^2)$ time complexity of strong graph state simulation (with phase) in [24].

THEOREM 6.3. *Let G be a graph with n vertices and a tree decomposition of G with width τ is given. Then the strong/weak simulation of $|G\rangle$ for $k \in \mathbb{N}$ amplitudes/samples could be solved in $O(n\tau^{\omega-1} + kn\tau^{\omega-2})$ time.*

Proof. By Lemma 6.2, each vertex v measured in Z basis could be preprocessed efficiently. In detail, suppose G has n vertices and m edges, and k vertices are measured in Z basis. Then we can compute in $O(n + m)$ time that,

$$(6.1) \quad \langle x | U_{\text{base}} | G \rangle = 2^{-k/2} \langle x' | H^{\otimes(n-k)} \check{Z}^d | G' \rangle,$$

where $d \in \mathbb{Z}_4^{n-k}$ and G' is the graph after deleting the k vertices measured in Z basis. Hence, strong and weak simulation of graph state $|G\rangle$ are reduced to strong and weak simulation of the phased graph state $|A\rangle = \check{Z}^d |G'\rangle$ respectively. Then the theorem follows from Theorem 5.5 and Theorem 5.4. \square

Also, we note that our algorithm can be used to simulate planar Clifford circuits studied in [20]. In particular, since our algorithm matches the complexity of graph state simulation in [20], it can be used in the proof of Theorem 7 in [20] to get the same $O(n^{\omega/2} d^\omega)$ complexity for simulating n -qubit depth- d planar Clifford circuit.

6.2. Clifford circuit simulation. In this section, we give the time complexities of our Clifford circuit simulation algorithm and compare it with related works. Combining Lemma 3.4 with the phased graph state simulation algorithms in section 5 gives the following theorem.

THEOREM 6.4. *Let U be a Clifford circuit with n qubits and m gates, each of which acts on at most 2 qubits, for $m = \Omega(n)$, and a tree decomposition of the circuit with width τ is given. Then strong/weak simulation of U for $k \in \mathbb{N}$ amplitudes/samples could be solved in $O(m\tau^{\omega-1} + \min(km\tau^{\omega-2}, mn\tau^{\omega-2} + kn^{\omega-1}))$ time.*

Proof. By Lemma 3.4, the circuit simulation problem can be reduced to a phased graph state simulation problem with $N = O(m + n)$ vertices. Further, a tree decomposition of the phased graph state of width at most τ can be obtained in linear time. Also, note that the number of unfixed output bits of this phased graph state, i.e. ℓ as defined in Theorem 5.4, is exactly n because it corresponds to the output qubits of the circuit. Then Theorem 5.5 and Theorem 5.4 gives the desired complexities stated in the theorem. \square

For any circuit as defined in Theorem 6.4, a tree decomposition of width at most $O(n)$ could always be obtained by dividing the gates into m/n consecutive parts such that each part is only connected to its preceding and subsequent parts. Then we have the following corollary.

COROLLARY 6.5. *Let U be a Clifford circuit with n qubits and m gates, each of which acts on at most 2 qubits, for $m = \Omega(n)$. Then strong/weak simulation of U for $k \in \mathbb{N}$ amplitudes/samples could be solved in $O(mn^{\omega-1} + kn^{\omega-1})$ time.*

This improves the result of quadratic form expansion method [15]. For weak simulation with many samples, the tableau method with Pauli frame propagation implemented in the Stim library [19] would take $O(n^\omega + km)$, and our algorithm can perform better when $m \gg n^{\omega-1}$ and $k \gg m$. When comparing with the quadratic-form-expansion methods, our algorithm is faster due to the usage of fast matrix multiplication. Table 6.1 compares the time complexity for strong and weak simulation in detail.

We note that the graph state simulation algorithm in [20] and [24] can also be applied to the graph given by our circuit-to-graph reduction in section 3 to solve single amplitude/sample strong/weak simulation of Clifford circuits. If the tree decomposition of width $O(n)$ is used, the runtime of that would be $O(mn^2)$ for strong simulation and $O(mn^{\omega-1})$ for weak simulation. In comparison, our algorithm matches

Methods	Strong simulation	Weak simulation
Tableau [1, 20]	$O(mn + kn^\omega)$	$O(mn + kn^\omega)$
Tableau with Pauli frame [19]	-	$O(n^\omega + km)$
Quadratic form expansions [15]	$O(mn^2 + kn^{\omega-1})$	$O(mn^2 + kn^2)$
This work	$O(mn^{\omega-1} + kn^{\omega-1})$	$O(mn^{\omega-1} + kn^{\omega-1})$

TABLE 6.1

Time complexity of strong simulation of Clifford circuits, where m is number of gates, n is number of qubits, k is number of amplitudes/samples for strong/weak simulation. Note that: (i) Fast matrix multiplication in sub-cubic time is assumed when possible. (ii) Ref. [15] mainly focuses on weak simulation, and the complexity of quadratic form expansions for strong simulation in the table is obtained by evaluating (2.1) directly using fast matrix multiplication.

the complexity for weak simulation and improves strong simulation in a similar way as in graph state simulation discussed in subsection 6.1.

6.3. Clifford+T circuit simulation. General quantum circuit can be represented by Clifford gates and T gates, where $T = R_z(\pi/4)$. Our techniques can also be used to simulate Clifford+T circuits by applying the stabilizer rank decomposition of non-Clifford states [6]. Such decompositions are defined as follows,

$$|T\rangle^{\otimes t} = \left(\bigcirc_{\pi/4} \right)^{\otimes t} = \sum_{j=1}^r \alpha_j |\phi_j\rangle,$$

where $\alpha_j \in \mathbb{C}$ are coefficients and $|\phi_j\rangle$ are Clifford states. The smallest possible r is called the stabilizer rank of $|T\rangle^{\otimes t}$ and it is known that $r \leq 2^{0.3963t}$ [30].

In particular, consider a quantum circuit U on n qubits with m Clifford gates and t T gates. By Lemma 3.4, we can represent $\langle b|U|0^n\rangle$ as a graph-like ZX diagram, and the phases of its nodes are multiples of $\pi/4$. For each node with phase $\pi/4$ or $3\pi/4$, we apply the following equality:

$$(6.2) \quad \begin{array}{c} \vdots \\ \vdots \\ \vdots \end{array} \bigcirc_{\pi/4} = \begin{array}{c} \vdots \\ \vdots \\ \vdots \end{array} \begin{array}{c} \bigcirc \\ \square \\ \bigcirc \\ \square \\ \bigcirc \\ \square \end{array} \bigcirc_{\pi/4}, \quad \begin{array}{c} \vdots \\ \vdots \\ \vdots \end{array} \bigcirc_{3\pi/4} = \begin{array}{c} \vdots \\ \vdots \\ \vdots \end{array} \begin{array}{c} \bigcirc \\ \square \\ \bigcirc \\ \square \\ \bigcirc \\ \square \end{array} \bigcirc_{\pi/2} \bigcirc_{\pi/4}.$$

In this way, the resulting ZX diagram can be divided into two parts: one contains $O(n + m)$ nodes with phase being multiples of $\pi/2$, and the other contains the new nodes introduced by (6.2), as depicted below.

$$(6.3) \quad \langle b|U|0^n\rangle = \begin{array}{c} \boxed{\kappa} \\ \vdots \\ \boxed{\kappa} \end{array} \begin{array}{c} \square \\ \vdots \\ \square \end{array} \begin{array}{c} \bigcirc \\ \vdots \\ \bigcirc \end{array} \begin{array}{c} \square \\ \vdots \\ \square \end{array} \begin{array}{c} \bigcirc_{\pi/4} \\ \vdots \\ \bigcirc_{\pi/4} \end{array}$$

We note that the first part of the diagram, labeled by κ , inherits the graph structure of U , while the second part the diagram represents $|T\rangle^{\otimes t}$ up to local Clifford gates. In this way, non-Clifford circuits can be reduced to weighted sum of Clifford circuits.

$$(6.4) \quad (6.3) = \sum_{j=1}^r \alpha_j \left(\begin{array}{c} \boxed{\kappa} \\ \vdots \\ \boxed{\kappa} \end{array} \begin{array}{c} \square \\ \vdots \\ \square \end{array} \begin{array}{c} \bigcirc \\ \vdots \\ \bigcirc \end{array} \begin{array}{c} \square \\ \vdots \\ \square \end{array} \boxed{\phi_j} \right)$$

Here, ϕ_j represents the ZX diagram representing the Clifford terms given by the stabilizer decomposition of $|T\rangle^{\otimes t}$.

Ignoring the edges between κ and ϕ_j , let the matrix representation of κ and ϕ_j be $\langle y^{(\kappa)} | H^{\otimes n} | A^{(\kappa)} \rangle$ and $\langle y^{(\phi_j)} | H^{\otimes n} | A^{(\phi_j)} \rangle$ respectively. Then the matrix representation of each term in (6.4) can be written as $\langle x^{(j)} | H^{\otimes n} | A^{(j)} \rangle$, where

$$A^{(j)} = \begin{bmatrix} A^{(\kappa)} & B^{(j)} \\ (B^{(j)})^T & A^{(\phi_j)} \end{bmatrix}, \quad x^{(j)} = \begin{bmatrix} y^{(\kappa)} \\ y^{(\phi_j)} \end{bmatrix},$$

and $B^{(j)}$ encodes t edges between κ and ϕ_j . Moreover, one can assume $A^{(\kappa)}$ is full rank by flipping any diagonal of it at the cost of introducing an extra dummy node in a similar way as in (6.2),

$$(6.5) \quad \begin{array}{c} \vdots \\ \circlearrowleft \beta \end{array} = \begin{array}{c} \vdots \\ \circlearrowleft \alpha \end{array} \text{---} \square \text{---} \square \text{---} \square \text{---} \circlearrowright \pi/2, \quad \text{where } \beta = \alpha + \pi/2.$$

Therefore, (6.4) could be evaluated by solving strong simulation problem for each $|A^{(j)}\rangle$. Note that each $A^{(\phi_j)}$ has $O(t)$ rows/columns because $|\phi_j\rangle$ can be represented as a graph state with local Clifford gates [37]. Since $A^{(\kappa)}$ is shared among all r terms, one only need to calculate LDL decomposition of $A^{(\kappa)}$ once. For each $j = 1, \dots, r$, we can compute the Schur complement of prefactorized $A^{(\kappa)}$ in $O(\text{nnz}(L^{(\kappa)}) + \text{nnz}(A^{(\kappa)}))$ time. So the overall time complexity is given by $O(T_{LDL}(A^{(\kappa)}) + r \cdot (\text{nnz}(L^{(\kappa)}) + \text{nnz}(A^{(\kappa)}) + t^\omega))$. This is summarized in the following theorem.

THEOREM 6.6. *Let U be a quantum circuit on n qubits represented by m Clifford gates and t T gates, r be the stabilizer rank of $|T\rangle^{\otimes t}$, and G be the graph representing structure of U . Let A be the matrix representing the Clifford part of the circuit and (P, L, D) be an LDL decomposition of A . Then the amplitude $\langle b|U|0^n \rangle$ for arbitrary binary string b can be evaluated in $O(T_{LDL}(A) + r \cdot (\text{nnz}(L) + \text{nnz}(A) + t^\omega))$ time, where $T_{LDL}(A)$ is the time complexity of computing LDL decomposition of A .*

This algorithm achieves better performance than naively simulating r Clifford circuits. In comparison, the previous work [7] approximates $|\langle b|U|0^n \rangle|^2$ with relative error ϵ and failure probability p_f in $O(\text{poly}(n, m) + rt^3\epsilon^{-2}p_f^{-1})$ time. Our algorithm utilizes fast matrix multiplication, runs deterministically and also computes the exact amplitude with phase. Further, for n -qubit planar circuits of depth d and t T gates as defined in [20, 24]⁴, the tree width is bounded by \sqrt{nd} . Hence, our algorithm runs in time $O(n^{(\omega+1)/2}d^\omega + r(n^{3/2}d + t^\omega))$, which generally improves the time complexity $O(r(n^{3/2}t^6d^3))$ achieved in [24, Theorem 33]. Finally, we note that this strong simulation algorithm can also be used for weak simulation using the gate-by-gate sampling method [9].

7. Other applications. In this section, we discuss other applications of our results. In subsection 7.1, we show that our result allows a new characterization of locally Clifford (LC) equivariant graph states, which leads to a linear bound of the diameter of each graph state orbit [2]. In subsection 7.2, we present an efficient protocol to learn graph states whose adjacency matrices are low rank.

⁴Planar circuits are circuits where two-qubit gates are applied on edges of a planar graph formed by qubits.

7.1. Local equivalence of graph states. Let \mathbb{Y}_2 be the set of the 2-by-2 Clifford unitaries. Two quantum states $|\psi\rangle$ and $|\phi\rangle$ are locally Clifford equivalent (LC-equivalent) iff

$$\exists U_1, \dots, U_n \in \mathbb{Y}_2, \text{ such that } |\psi\rangle = \left(\bigotimes_{i=1}^n U_i \right) |\phi\rangle.$$

THEOREM 7.1. *Two n qubit graph states are LC-equivalent iff, for some ordering of vertices, their adjacency matrices A and B satisfy*

$$\exists u, v \in \mathbb{F}_2^n, k \in \{0, \dots, n\}, \text{ such that } A + D(u) = \omega_1(\Gamma_k(B + D(v))).$$

Proof. For brevity, we use the notation $|\psi\rangle \propto |\phi\rangle$ to mean $\exists \alpha \in \mathbb{C}, |\alpha| = 1$ such that $|\psi\rangle = \alpha |\phi\rangle$. We denote the elementwise product of two vectors u and v as $u \circ v$.

Any one-qubit Clifford unitary may be represented, for some $a, b, c \in \{0, 1, 2, 3\}$, as

$$U \propto \check{Z}^a \check{X}^b \hat{Z}^c,$$

which is sometimes referred to as the Euler decomposition of the gate. We provide a proof that the Clifford Euler decomposition always exists in [Lemma B.1](#) in [section B](#). We further decompose $\check{X}^b = X^{\omega_2(b)} (\check{Z} H \check{Z})^{\omega_1(b)}$, and use the canonical form $a', b' \in \mathbb{F}_2, c', d' \in \{0, 1, 2, 3\}$,

$$U \propto \check{Z}^{c'} X^{a'} H^{b'} \hat{Z}^{d'}$$

Hence, for a general local unitary transformation given by one-qubit unitaries U_1, \dots, U_n , we may find $\hat{u}, \bar{v} \in \{0, 1, 2, 3\}^n, p, q \in \mathbb{F}_2^n$, such that,

$$(7.1) \quad \left(\bigotimes_{i=1}^n U_i \right) |B\rangle \propto \check{Z}^{\hat{u}} X^q H^p |B + D(\bar{v})\rangle$$

Let $S = \{i, p_i = 1, i \in \{1, \dots, n\}\}$, $s = |S|$ and consider a subset $S' \subseteq S$ such that S' is of maximal size $s' = |S'|$ and the set of indices in S' correspond to linearly independent columns/rows of $\omega_1(B + D(\bar{v}))$. Assume wlog the columns/rows of $B + D(\bar{v})$ are ordered as $S' \prec \{1, \dots, n\} \setminus S \prec S \setminus S'$, so $S' = \{1, \dots, s'\}$. Then, by [Lemma 4.2](#), for some $x, z \in \mathbb{F}_2^n$ (with only the first s' elements potentially nonzero),

$$H^{\otimes s'} \otimes I^{\otimes(n-s')} |B + D(\bar{v})\rangle \propto X^x Z^z |\Gamma_{s'}(B + D(\bar{v}))\rangle,$$

hence

$$(7.2) \quad H^p |B + D(\bar{v})\rangle = (I^{\otimes(n-(s-s'))} \otimes H^{\otimes(s-s')}) (H^{\otimes s'} \otimes I^{\otimes(n-s')} |B + D(\bar{v})\rangle)$$

$$(7.3) \quad \propto (I^{\otimes(n-(s-s'))} \otimes H^{\otimes(s-s')}) X^x Z^z |\Gamma_{s'}(B + D(\bar{v}))\rangle$$

$$(7.4) \quad = X^x Z^z (I^{\otimes(n-(s-s'))} \otimes H^{\otimes(s-s')}) |\Gamma_{s'}(B + D(\bar{v}))\rangle.$$

However, note that the bottom right $(s - s') \times (s - s')$ block of $|\Gamma_{s'}(B + D(\bar{v}))\rangle$ must be zero modulo two, as the last columns are linearly dependent on the first s' . Hence, we may apply [Lemma 4.4](#) to

$$(I^{\otimes(n-(s-s'))} \otimes H^{\otimes(s-s')}) |\Gamma_{s'}(B + D(\bar{v}))\rangle,$$

and observe that if $s > s'$, the magnitude of the amplitudes of the above state are not constant (differ from that of a graph state). Hence, if $s > s'$,

$$(7.5) \quad |\langle A | \left(\bigotimes_{i=1}^n U_i \right) |B\rangle| = |\langle A + D(\hat{u} + 2z) | X^x |\Gamma_{s'}(B + D(\bar{v}))\rangle| \neq 1,$$

since, we have that for any phased graph state $|R\rangle$, any any $j \in \{0, \dots, n\}$,

$$(7.6) \quad X^{(j)} |R\rangle \propto \sum_{x \in \mathbb{F}_2^n} i^{-(x-e_j)^T R(x-e_j)} \propto \sum_{x \in \mathbb{F}_2^n} i^{-x^T (R+2D(r_j))x} = |R + 2D(r_j)\rangle,$$

where r_j is the j th row/column of R . Hence, $\exists \bar{u} \in \{0, 1, 2, 3\}^n$, such that

$$\langle A + D(\hat{u} + 2z) | X^x \propto \langle A + D(\bar{u}) |.$$

Therefore, we must have $S = S'$.

We have shown that $A + D(\bar{u})$ and $\Gamma_s(B + D(\bar{v}))$ can differ only in the second bit of the diagonal. Choosing $\omega_2(\bar{u}) \neq 0$ has no affect on $\omega_1(\Gamma_s(B + D(\bar{v})))$ and hence no affect on the graph state we transform to (although we must ensure $\omega_2(\bar{u})$ and $\omega_2(\bar{v})$ are 0, so that we do transform to a graph state, which is always possible with appropriate local unitary transformations). Hence, we have shown that all LC-equivalent graph states may be related by a partial pivot transform modulo 2, with appropriate change to the diagonal before and after. Specifically, we have shown that given LC-equivalence of two graph states, we can directly derive the relation in the Lemma with $u = \omega_1(\bar{u})$ and $v = \omega_1(\bar{v})$. \square

The set of n -qubit graph states can be viewed as a group with vertex complementation as the group operation. Then the orbits of this group are classes of LC-equivalent graph states and the diameter of an orbit gives the the smallest number of vertex complementations needed to transform one graph state in the orbit to another. It has been heuristically observed that the diameter of a graph state orbit is strongly correlated to entanglement measure (i.e. Schmidt measure) of graph states [2]. However, to the best of our knowledge, theoretical bounds of such diameters are not yet studied in the literature. The theorem below, as a consequence of [Theorem 7.1](#), provides a general bound of diameter for all graph state orbits. Here, we consider graph states with unlabeled vertices, which means isomorphic graphs are considered equivalent.

THEOREM 7.2. *The LC-equivalence diameter of any n -qubit graph state orbit with unlabeled vertices is at most $\lfloor 3n/2 \rfloor$.*

Proof. Consider any two LC-equivalent graph states with adjacency matrices A and B . By [Theorem 7.1](#), there exist some $u, v \in \mathbb{F}_2^n$ and $k \in \{0, \dots, n\}$ such that in some ordering of vertices,

$$(7.7) \quad |A + D(u)\rangle = |\omega_1(\Gamma_k(B + D(v)))\rangle.$$

The off-diagonals of $A + D(u)$ and $\omega_1(\Gamma_k(B + D(v)))$ must match, so we have

$$A = O(\Gamma_k(B + D(v))).$$

Further, by definition of Gauss-Jordan process, the RHS can be viewed as the resulting graph after applying a series of disjoint vertex or edge complementations on the graph represented by B . Since each edge complementation can be represented by three vertex complementations as stated in [Theorem 2.7](#), the graph A could be obtained by applying at most $\lfloor 3n/2 \rfloor$ vertex complementations on B . \square

7.2. Graph state learning. Quantum state learning is of great interest in order to understand complexity-theoretic properties of quantum states and experimentally characterize real-world quantum states [4]. In the setting of this problem, we are provided with a number of identical copies of some unknown quantum states $|\psi\rangle$, on which we can apply arbitrary circuits/measurements, and the goal is to obtain a mathematical representation of $|\psi\rangle$ using as few copies as possible. In this section, we consider the problem of learning graph states and provides an algorithm to learn the graph state efficiently if its adjacency matrix is low rank.

We take advantage of the fact that the measurement results of an n -qubit stabilizer state forms an affine subspace of \mathbb{F}_2^n , so learning the subspace could reduce the original state to a stabilizer state with fewer qubits [4, Theorem 3]. Although the measurement results of a graph state form the full space of \mathbb{F}_2^n (i.e. the amplitudes vector of any graph state has no zeros), our results for strong simulation of phased graph states allows similar ideas to be applied on graph states. This is detailed in the following lemma.

LEMMA 7.3. *Given an unknown n -qubit graph state $|G\rangle$, then one can compute a positive integer r and a circuit U composed of CNOT and X gates using $O(r \log \frac{1}{\delta})$ one-copy measurements of $|G\rangle$ such that the following is satisfied with probability at least $1 - \delta$,*

- r is exactly the rank of adjacency matrix of G ;
- $UH^{\otimes n}|\psi\rangle = |\phi\rangle \otimes |0^{n-r}\rangle$ for some r -qubit stabilizer state $|\phi\rangle$.

Proof. By Theorem 5.5, there exist $Q \in \mathbb{J}_r$, $A \in \mathbb{F}_2^{n \times r}$, $b \in \mathbb{F}_2^n$ such that

$$(7.8) \quad H^{\otimes n} |G\rangle = 2^{-r/2} \sum_{x \in \mathbb{F}_2^n} i^{x^T Q x} |\omega_1(Ax + b)\rangle.$$

Measuring (7.8) in computational basis outputs $\omega_1(Ax + b)$ for uniformly random $x \in \mathbb{F}_2^n$, so one can uniformly sample k vectors in $\text{span}(A)$ with $k + 1$ measurements.

Consider the algorithm that iteratively samples vectors $v^{(1)}, \dots, v^{(k)}$ from $\text{span}(A)$ and constructs $A^{(k)} = [v^{(1)} \ v^{(2)} \ \dots \ v^{(k)}]$ until $\text{rank}(A^{(k)}) = \text{rank}(A^{(k+s)})$ for $s = \lceil \log_2 \frac{1}{\delta} \rceil$. Let $r = \text{rank}(A^{(k)})$. Note that $k \leq rs$, so we need at most $O(r \log \frac{1}{\delta})$ one-copy measurements. Then we bound the failure probability. Note that the probability of a random vector falling in $\text{span}(A^{(k)})$ is $1/2^{r - \text{rank}(A^{(k)})}$. Let F denote the event when the algorithm fails – that is, $v^{(k+j)} \in \text{span}(A^{(k)})$ for all $j \in [s]$ and $\text{rank}(A^{(k)}) < r$. Then

$$(7.9) \quad p(F) = \left(\frac{1}{2^{r - \text{rank}(A^{(k)})}} \right)^s \leq \frac{1}{2^s} \leq \delta.$$

Next, we construct the circuit U . Assume WLOG that $A = \begin{bmatrix} A_1 \\ A_2 \end{bmatrix}$ for invertible $A_1 \in \mathbb{F}_2^{n \times n}$. Then

$$(7.10) \quad (7.8) = 2^{-r/2} \sum_{x \in \mathbb{F}_2^n} i^{x^T Q x} |\omega_1(A_1 x + b_1)\rangle \otimes |\omega_1(A_2 x + b_2)\rangle$$

$$(7.11) \quad = 2^{-r/2} \sum_{x \in \mathbb{F}_2^n} i^{x^T Q x} U |\omega_1(A_1 x + b_1)\rangle \otimes |0^{n-r}\rangle,$$

where U is a circuit that computes $\omega_1(A_2 x + b_2)$ in the last $n - r$ qubits using $\omega_1(A_1 x + b_1)$

b_1) from the first r qubits. In particular, for any $y \in \mathbb{F}_2^r$, $z \in \mathbb{F}_2^{n-r}$,

$$(7.12) \quad U |y\rangle \otimes |z\rangle = |y\rangle \otimes \left| z \oplus \omega_1(A_2 A_1^\#(y + b_1) + b_2) \right\rangle.$$

Note that U can be expressed using only CNOT and X gates and $U = U^{-1}$. Also, U commutes with $i^{x^T Q x}$, so (7.11) gives $U H^{\otimes n} |G\rangle = |\phi\rangle \otimes |0^{n-r}\rangle$, where

$$(7.13) \quad |\phi\rangle = 2^{-r/2} \sum_{x \in \mathbb{F}_2^r} i^{x^T Q x} |\omega_1(A_1 x + b_1)\rangle.$$

Note that $|\phi\rangle$ must be a stabilizer state because H and U are Clifford gates. \square

Then we have the following theorem to learn graph states with low-rank adjacency matrices efficiently.

THEOREM 7.4. *An unknown graph state whose adjacency matrix is of rank r can be learned using $O(r^2 + r \log \frac{1}{\delta})$ one-copy measurements, or $O(r \log \frac{1}{\delta})$ two-copy measurements, with probability at least $1 - \delta$.*

Proof. Combining Lemma 7.3 and the known techniques to learn r -qubit stabilizer state using $O(r^2)$ one-copy measurements [1] or $O(r)$ two-copy measurements [27] gives the theorem. \square

8. Conclusion. In this work, we present reductions from several quantum circuit simulation problems, including graph state simulation, Clifford circuit simulation, and Clifford+T circuit simulation, to the standard linear algebra problem known as LDL decomposition. In particular, we represent the problem as a modified adjacency matrix of some graph that inherits the structure of the original problem, such that the LDL decomposition of the matrix gives the simulation result. This relation is shown via an explicit formula for amplitudes of Hadamard-transformed phased graph state in Theorem 4.5. This result extends the application of standard linear algebra algorithms to the field of quantum circuit simulation. Based on this idea, we apply the tree-decomposition-based fast LDL decomposition [32] and derive algorithms for various simulation problems. We analyze the complexities of our algorithms and show improvements over state of arts in certain cases. Moreover, we show that our amplitudes formula has wider applications beyond simulation. In particular, we give a new characterization of LC-equivalent graph state based on the Gauss-Jordan process and discuss its implications for bounding the diameter of each graph state orbit. Also, we design a protocol to efficiently learn graph states with low-rank adjacency matrices based on the amplitudes formula. We believe that our work provides a new perspective on Clifford circuit simulation and opens up new possibilities for applying existing linear algebra techniques to quantum circuit simulation.

Acknowledgments. The authors acknowledge support from the NSF QLCI-HQAN Award No. 2016136.

REFERENCES

- [1] S. AARONSON AND D. GOTTESMAN, Improved simulation of stabilizer circuits, Physical Review A—Atomic, Molecular, and Optical Physics, 70 (2004), p. 052328.
- [2] J. C. ADCOCK, S. MORLEY-SHORT, A. DAHLBERG, AND J. W. SILVERSTONE, Mapping graph state orbits under local complementation, Quantum, 4 (2020), p. 305.
- [3] S. ANDERS AND H. J. BRIEGEL, Fast simulation of stabilizer circuits using a graph-state representation, Phys. Rev. A, 73 (2006), p. 022334, <https://doi.org/10.1103/PhysRevA.73.022334>, <https://link.aps.org/doi/10.1103/PhysRevA.73.022334>.

- [4] A. ANSHU AND S. ARUNACHALAM, A survey on the complexity of learning quantum states, *Nature Reviews Physics*, 6 (2024), pp. 59–69.
- [5] A. BOUCHET, Graphic presentations of isotropic systems, *Journal of Combinatorial Theory, Series B*, 45 (1988), pp. 58–76.
- [6] S. BRAVYI, D. BROWNE, P. CALPIN, E. CAMPBELL, D. GOSSET, AND M. HOWARD, Simulation of quantum circuits by low-rank stabilizer decompositions, *Quantum*, 3 (2019), p. 181.
- [7] S. BRAVYI AND D. GOSSET, Improved classical simulation of quantum circuits dominated by clifford gates, *Physical review letters*, 116 (2016), p. 250501.
- [8] S. BRAVYI, D. GOSSET, AND R. KÖNIG, Quantum advantage with shallow circuits, *Science*, 362 (2018), pp. 308–311.
- [9] S. BRAVYI, D. GOSSET, AND Y. LIU, How to simulate quantum measurement without computing marginals, *Physical Review Letters*, 128 (2022), p. 220503.
- [10] A. R. CALDERBANK, E. M. RAINS, P. W. SHOR, AND N. J. SLOANE, Quantum error correction and orthogonal geometry, *Physical Review Letters*, 78 (1997), p. 405.
- [11] N. CLAUDET AND S. PERDRIX, Local equivalence of stabilizer states: a graphical characterisation, arXiv preprint arXiv:2409.20183, (2024).
- [12] B. COECKE AND R. DUNCAN, Interacting quantum observables, in *International Colloquium on Automata, Languages, and Programming*, Springer, 2008, pp. 298–310.
- [13] C. DAMM, Problems complete for $\oplus 1$, in *International Meeting of Young Computer Scientists*, Springer, 1990, pp. 130–137.
- [14] L. E. DANIELSEN, On self-dual quantum codes, graphs, and boolean functions, arXiv preprint quant-ph/0503236, (2005).
- [15] N. DE BEAUDRAP AND S. HERBERT, Fast stabiliser simulation with quadratic form expansions, *Quantum*, 6 (2022), p. 803.
- [16] J. DEHAENE AND B. DE MOOR, Clifford group, stabilizer states, and linear and quadratic operations over $\text{GF}(2)$, *Physical Review A*, 68 (2003), p. 042318.
- [17] R. DUNCAN, A. KISSINGER, S. PERDRIX, AND J. VAN DE WETERING, Graph-theoretic Simplification of Quantum Circuits with the ZX-calculus, *Quantum*, 4 (2020), p. 279, <https://doi.org/10.22331/q-2020-06-04-279>, <https://doi.org/10.22331/q-2020-06-04-279>.
- [18] R. DUNCAN AND S. PERDRIX, Pivoting makes the zx-calculus complete for real stabilizers, arXiv preprint arXiv:1307.7048, (2013).
- [19] C. GIDNEY, Stim: a fast stabilizer circuit simulator, *Quantum*, 5 (2021), p. 497.
- [20] D. GOSSET, D. GRIER, A. KERZNER, AND L. SCHAEFFER, Fast simulation of planar Clifford circuits, *Quantum*, 8 (2024), p. 1251.
- [21] D. GOTTESMAN, Class of quantum error-correcting codes saturating the quantum Hamming bound, *Physical Review A*, 54 (1996), p. 1862.
- [22] D. GOTTESMAN, The Heisenberg representation of quantum computers, arXiv preprint quant-ph/9807006, (1998).
- [23] A. HADZIHASANOVIC, K. F. NG, AND Q. WANG, Two complete axiomatisations of pure-state qubit quantum computing, in *Proceedings of the 33rd annual ACM/IEEE symposium on logic in computer science*, 2018, pp. 502–511.
- [24] A. KERZNER, Clifford simulation: Techniques and applications, master’s thesis, University of Waterloo, 2021.
- [25] B. A. LAMACCHIA AND A. M. ODLYZKO, Solving large sparse linear systems over finite fields, in *Advances in Cryptology-CRYPTO’90: Proceedings 10*, Springer, 1991, pp. 109–133.
- [26] I. L. MARKOV AND Y. SHI, Simulating quantum computation by contracting tensor networks, *SIAM Journal on Computing*, 38 (2008), pp. 963–981.
- [27] A. MONTANARO, Learning stabilizer states by bell sampling, arXiv preprint arXiv:1707.04012, (2017).
- [28] M. A. MORRISON AND J. BRILLHART, A method of factoring and the factorization of f_7 , *Mathematics of computation*, 29 (1975), pp. 183–205.
- [29] M. A. NIELSEN AND I. L. CHUANG, Quantum computation and quantum information, Cambridge university press, 2010.
- [30] H. QASSIM, H. PASHAYAN, AND D. GOSSET, Improved upper bounds on the stabilizer rank of magic states, *Quantum*, 5 (2021), p. 606.
- [31] R. RAUSSENDORF, D. E. BROWNE, AND H. J. BRIEGEL, Measurement-based quantum computation on cluster states, *Physical review A*, 68 (2003), p. 022312.
- [32] E. SOLOMONIK, Fast LDL factorization for dense and sparse symmetric matrices over an arbitrary field, arXiv preprint arXiv:2504.20305, (2025).
- [33] C. SPENGLER AND B. KRAUS, Graph-state formalism for mutually unbiased bases, *Physical Review A—Atomic, Molecular, and Optical Physics*, 88 (2013), p. 052323.
- [34] V. STRASSEN, Gaussian elimination is not optimal, *Numerische mathematik*, 13 (1969), pp. 354–

- [35] M. J. TSATSOMEROS, Principal pivot transforms: properties and applications, Linear Algebra and its Applications, 307 (2000), pp. 151–165.
- [36] M. VAN DEN NES, Classical simulation of quantum computation, the Gottesman-Knill theorem, and slightly beyond, Quantum Information & Computation, 10 (2010), pp. 258–271.
- [37] M. VAN DEN NEST, J. DEHAENE, AND B. DE MOOR, Graphical description of the action of local clifford transformations on graph states, Phys. Rev. A, 69 (2004), p. 022316, <https://doi.org/10.1103/PhysRevA.69.022316>, <https://link.aps.org/doi/10.1103/PhysRevA.69.022316>.
- [38] V. V. WILLIAMS, Y. XU, Z. XU, AND R. ZHOU, New bounds for matrix multiplication: from alpha to omega, in Proceedings of the 2024 Annual ACM-SIAM Symposium on Discrete Algorithms (SODA), SIAM, 2024, pp. 3792–3835.
- [39] L. ZHAO, C. A. PÉREZ-DELGADO, AND J. F. FITZSIMONS, Fast graph operations in quantum computation, Physical Review A, 93 (2016), p. 032314.

Appendix A. Reducing stabilizer states to graph states. It is widely known that stabilizer states can always be represented as a graph state with local Clifford gates [37]. In this section, we list some useful operations on tableaux in [Algorithm A.1](#). Based on these operations, we provide [Algorithm A.2](#), which converts a stabilizer state in tableau representation into an XY-basis graph state up to bit flips. It takes as input the lower n rows of a tableau representation of a stabilizer state, and outputs a graph and three layers of Clifford gates, namely S^\dagger , H and X .

Appendix B. A canonical form of one-qubit Clifford gate. One-qubit Clifford gates can be generated by $\{\check{Z}, \check{X}\}$. Note that \check{Z}, \check{X} can be viewed as -90 degree rotations around z- or x-axis in Bloch sphere. Therefore, any such rotation can be represented in form $\check{Z}^a \check{X}^b \check{Z}^c$ for $a, b, c \in \mathbb{Z}_4$ using Euler angles of the rotation as presented in the following lemma.

LEMMA B.1. *Any one-qubit Clifford gate can be represented as $\check{Z}^a \check{X}^b \check{Z}^c$ for some $a, b, c \in \mathbb{Z}_4$.*

Proof. Consider an arbitrary one-qubit Clifford gate $U = \prod_i (\check{X}^{x_i} \check{Z}^{z_i})$ for $x_i, z_i \in \{0, 1, 2, 3\}$, which is a string of powers of \check{Z} or \check{X} . For any sub-string of form $\check{X}^a \check{Z}^b \check{X}^c$, one can apply one of the equalities below to replace it with $\check{Z}^{a'} \check{X}^{b'} \check{Z}^{c'}$.

$$(B.1) \quad \check{X} \check{Z}^2 \check{X} = \check{Z}^2$$

$$(B.2) \quad \check{X}^2 \check{Z}^b \check{X}^2 = \check{Z}^{b-2}, \quad b \in \{1, 3\}$$

$$(B.3) \quad \check{X}^a \check{Z}^b \check{X}^c = \check{Z}^c \check{X}^b \check{Z}^a, \quad a, b, c \in \{1, 3\}$$

More specifically,

- if any of a, b, c is 0, then it is trivial;
- if $b = 2$, applying (B.1) for a times gives $\check{Z}^b \check{X}^{c-a}$;
- if $b \in \{1, 3\}$ and either a or c is even, applying (B.2) for $a/2$ times (if a is even) or $c/2$ times (if c is even) gives $\check{Z}^{b-a} \check{X}^{c-a}$ or $\check{X}^{a-c} \check{Z}^{b-c}$ respectively;
- if $a, b, c \in \{1, 3\}$, applying (B.3) directly gives the desired form.

This process reduces the number of nonconsecutive \check{X} in the string by one and we can repeat it until there is only one \check{X} in the string, which have the form $\check{Z}^a \check{X}^b \check{Z}^c$ for $a, b, c \in \mathbb{Z}_4$. \square

Algorithm A.1 Basic tableau operations

procedure ROW_ADD($\tilde{Z}, \tilde{X}, r, i, j$) ▷ add j'th row to i'th row
 for $k=1, \dots, n$ **do**
 $\tilde{z}_{ik} := (\tilde{z}_{ik} + \tilde{z}_{jk}) \bmod 2$
 $\tilde{x}_{ik} := (\tilde{x}_{ik} + \tilde{x}_{jk}) \bmod 2$
 end for
 $r_i := (r_i + r_j + \lfloor (\sum_{k=1}^n f(g(\tilde{z}_{ik}, \tilde{x}_{ik}), g(\tilde{z}_{jk}, \tilde{x}_{jk}))) / 2 \rfloor) \bmod 2$, where

$$g(z, x) = x + 3z - 2zx$$

$$f(p_1, p_2) = \begin{cases} 0 & p_1 = 0 \text{ or } p_2 = 0 \\ (p_2 - p_1) \bmod 3 & \text{otherwise} \end{cases}$$

 ▷ $g(z, x)$ represents I, X, Y, Z as 0, 1, 2, 3 respectively
end procedure
procedure APPLY_H($\tilde{Z}, \tilde{X}, r, i$)
 Swap the i 'th column of \tilde{Z} and the i 'th column of \tilde{X}
 for $j=1, \dots, n$ **do**
 $r_j := (r_j + \tilde{z}_{ji}\tilde{x}_{ji}) \bmod 2$
 end for
end procedure
procedure APPLY_S($\tilde{Z}, \tilde{X}, r, i$)
 for $j=1, \dots, n$ **do**
 $r_j := (r_j + \tilde{z}_{ji}\tilde{x}_{ji}) \bmod 2$
 $\tilde{z}_{ji} := (\tilde{z}_{ji} + \tilde{x}_{ji}) \bmod 2$
 end for
end procedure
procedure APPLY_CZ($\tilde{Z}, \tilde{X}, r, a, b$)
 for $j=1, \dots, n$ **do**
 $r_j := (r_j + \tilde{x}_{ja}\tilde{x}_{jb}(\tilde{z}_{ja} + \tilde{z}_{jb})) \bmod 2$
 $\tilde{z}_{ja} := (\tilde{z}_{ja} + \tilde{x}_{jb}) \bmod 2$
 $\tilde{z}_{jb} := (\tilde{z}_{jb} + \tilde{x}_{ja}) \bmod 2$
 end for
end procedure

Algorithm A.2 $[G, a, b, c] = \text{stabilizers_to_graph}(\tilde{Z}, \tilde{X}, r)$

Require: $\tilde{Z}, \tilde{X} \in \{0, 1\}^{n \times n}$, $r \in \{0, 1\}^n$, $(\tilde{Z}, \tilde{X}, r)$ represents stabilizers of $|\psi\rangle$

Ensure: $a, b, c \in \{0, 1\}^n$ such that $|\psi\rangle = \left(\bigotimes_{j=1}^n X^{c_j} H^{a_j} (S^\dagger)^{b_j} \right) |G\rangle$

Initialize a, b as zero vectors

Initialize permutation p as $(1, \dots, n)$

procedure COLUMN_SWAP(i, j)

Swap the i 'th and j 'th entry of a, b, r, p respectively

Swap the i 'th and j 'th column of \tilde{Z}, \tilde{X} respectively

end procedure

for $i = 1, \dots, n$ **do**

▷ forward elimination

if $\tilde{X}[i, i :]$ are all zeros **then**

Find the index k of the first nonzero in $\tilde{Z}[i, i :]$

APPLY_H($\tilde{Z}, \tilde{X}, r, i + k - 1$)

$a_i := a_i + 1$

else

Find the index k of the first nonzero in $\tilde{X}[i, i :]$

end if

COLUMN_SWAP($i, i + k - 1$)

for $j = i + 1, \dots, n$ **do**

ROW_ADD($\tilde{Z}, \tilde{X}, r, j, i$)

end for

end for

for $i = n, \dots, 1$ **do**

▷ backward substitution

for $j = 1, \dots, i$ **do**

if $\tilde{x}_{ij} \neq 0$ **then**

ROW_ADD($\tilde{Z}, \tilde{X}, r, j, i$)

end if

end for

end for

for $i = 1, \dots, n$ **do**

▷ zero out diagonals of \tilde{Z}

if $\tilde{z}_{ii} \neq 0$ **then**

APPLY_S($\tilde{Z}, \tilde{X}, r, i$)

$b_i := b_i + 1$

end if

end for

Compute the inverse permutation p^{-1} of p

Permute a, b, r with p^{-1}

Permute both rows and columns of \tilde{Z} with p^{-1}

Let $c := r$ and G be the graph represented by adjacency matrix \tilde{Z}

return G, a, b, c
